

高流强重离子加速器装置 (*High Intensity Heavy-ion Accelerator Facility*: HIAF) 上的核物理研究

孙志宇

中国科学院近代物理研究所

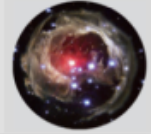
- HIAF简介
- HIAF上计划开展的核物理研究工作
- HIAF建设进展
- 总结

Challenges in MODERN NUCLEAR PHYSICS

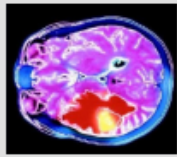
Quest for a UNIFIED DESCRIPTION of ALL Nuclei

INTERDISCIPLINARITY

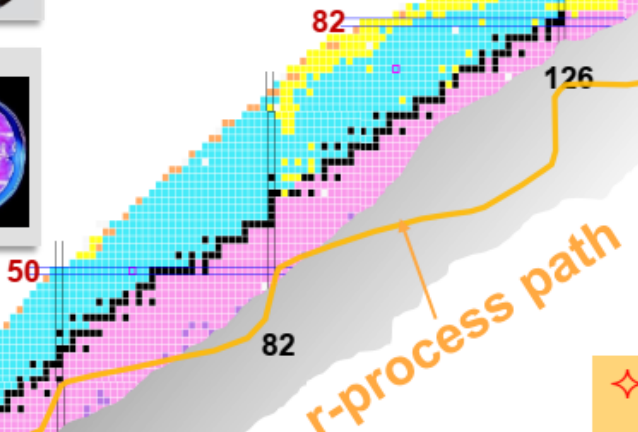
Astrophysics
Nucleosynthesis



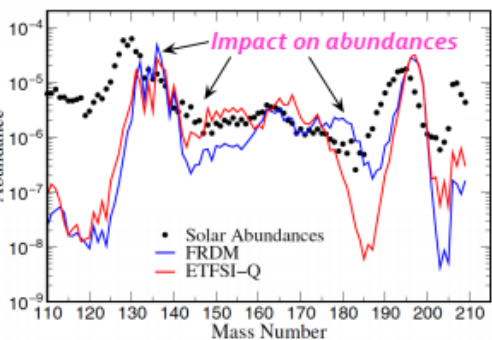
Applications
Radioisotopes,
Reactors, ...



Proton Z



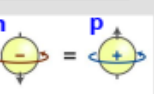
Element
ABUNDANCES



Neutron number N

BASIC SCIENCE

Many Body
Finite Quantum
System



Symmetry
Principle

◆ SHELL STRUCTURE
(Magic Numbers)

◆ SHAPES

◆ EXCITATIONS

研究目标

- 核力的本质，原子核的统一描述
- 原子核的存在极限
- 化学元素的起源
- QCD相结构与低温高密核物质的性质
-

手段

探索未知领域
更强的重离子束流
领先的探测装置

需要建设新一代的高流
强重离子加速器装置



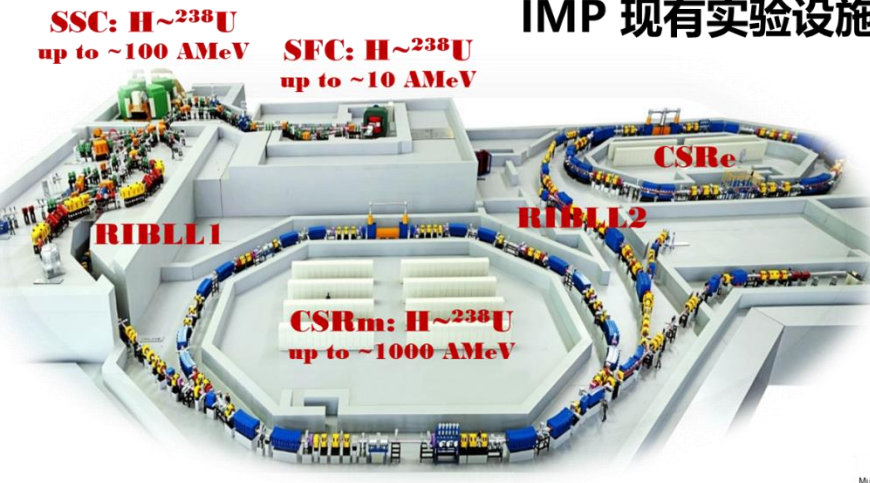
HIAF简介



北
南

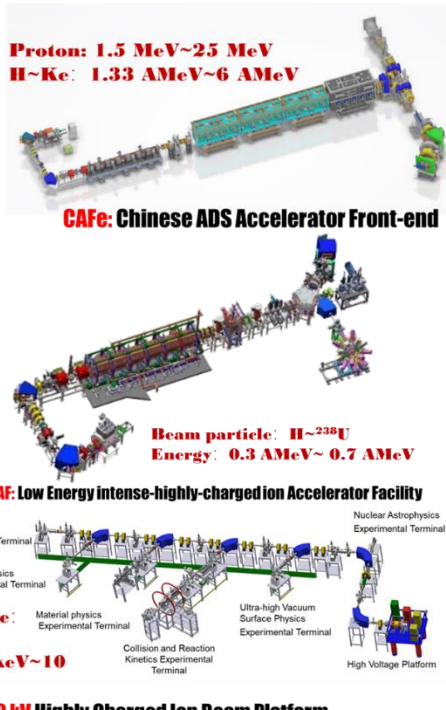


中国科学院近代物理研究所
Institute of Modern Physics, Chinese Academy of Sciences



EBIS: super low energy heavy ion experiment platform

IMP 现有实验设施





HIAF简介



2010

May, 2011

December, 2015

April, 2017

2018

提交HIAF
项目建议书HIAF进入“十二五”
候选项目名单（共16项）建设地点最终确定，HIAF
项目得到政府批准立项HIAF项目可
研报告获批12月23号，HIAF
建设正式启动

强流重离子加速器装置 (HIAF) 国际上脉冲束流强度最高的重离子加速器装置

定位于重离子物理及应用研究

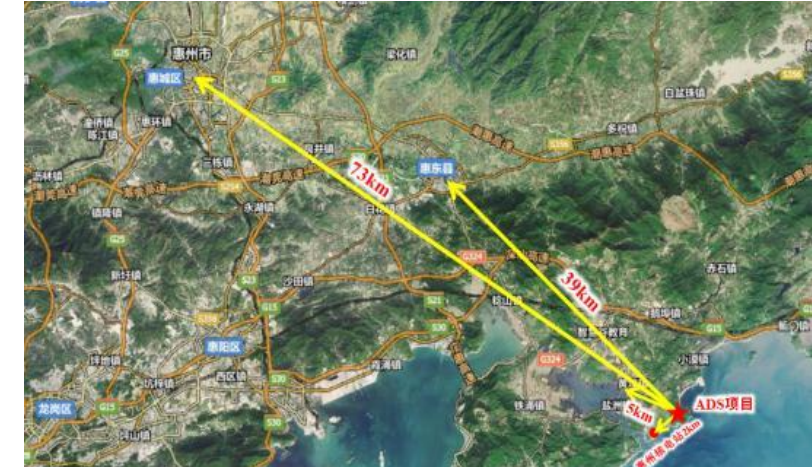
科学目标：

- 1) 认识原子核中的有效相互作用
- 2) 理解宇宙中从铁到铀重元素的来源
- 3) 研究高能量密度物理性质
- 4) 空间辐射环境地面模拟
- 5)

“十二五”
国家重大科
技基础设施

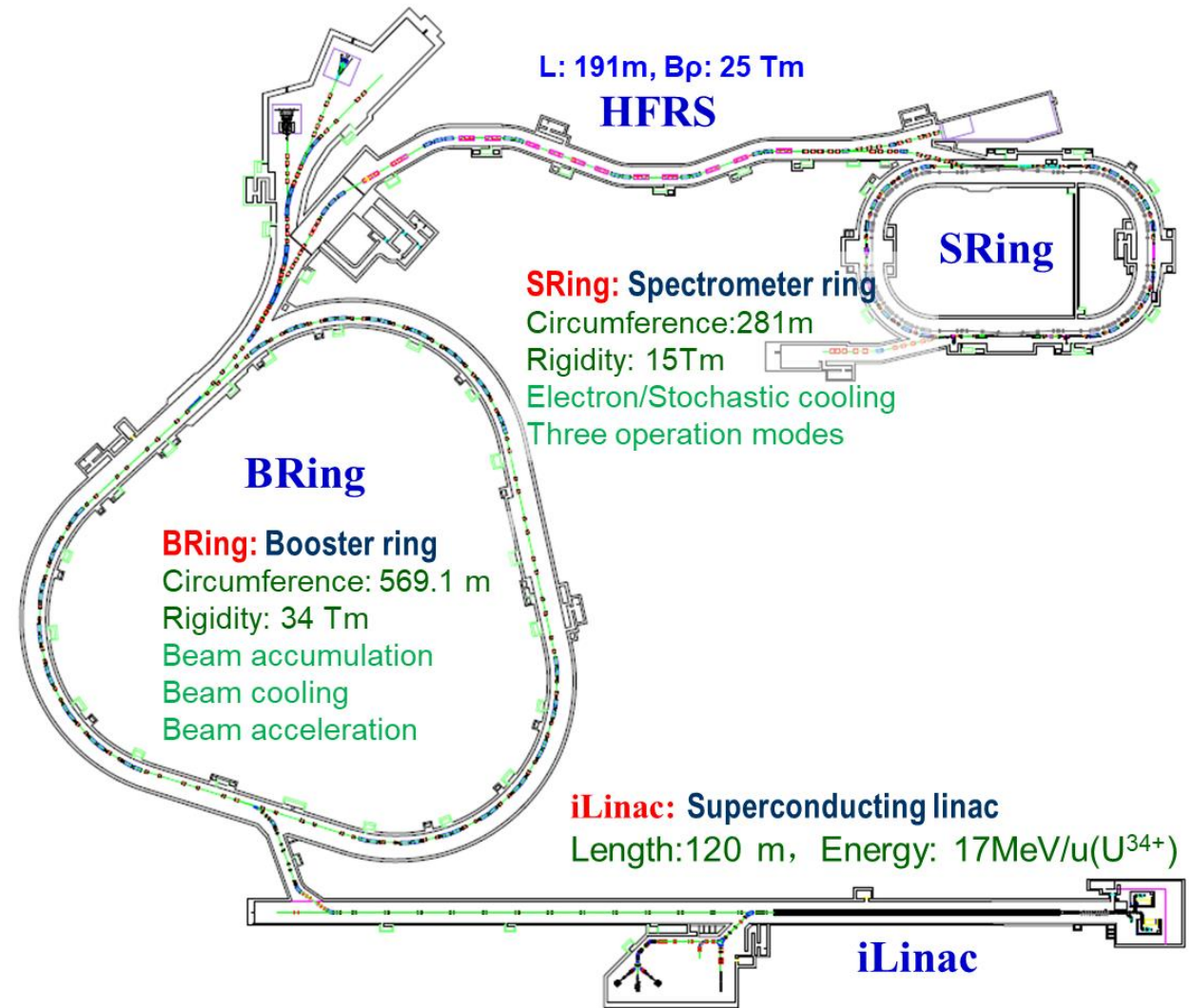
国家投资16.7亿元
预计建设时间7年！

■坐落地点：广东省惠州市黄埠镇





■ HIAF 主要参数



	SECR	iLinac	BRing	HFRS	SRing
Length / circumference (m)	---	114	569	192	277
Final energy of U (MeV/u)	0.014 (U^{35+})	17 (U^{35+})	835 (U^{35+})	800 (U^{92+})	800 (U^{92+})
Max. magnetic rigidity (Tm)	---	---	34	25	15
Max. beam intensity of U	50 p μ A (U^{35+})	28 p μ A (U^{35+})	2×10^{11} ppp (U^{35+})	-----	10^{10} ppp (U^{92+})
Operation mode	DC	CW or pulse	fast ramping (12T/s, 3Hz)	Momentum-resolution 1100	DC, deceleration
Emittance or Acceptance (H/V, $\pi \cdot \text{mm} \cdot \text{mrad}$, dp/p)		5 / 5	200/100, 0.5%	$\pm 30\text{mrad}(H)/\pm 15\text{mrad}(V), \pm 2\%$	40/40, 1.5% (normal mode)

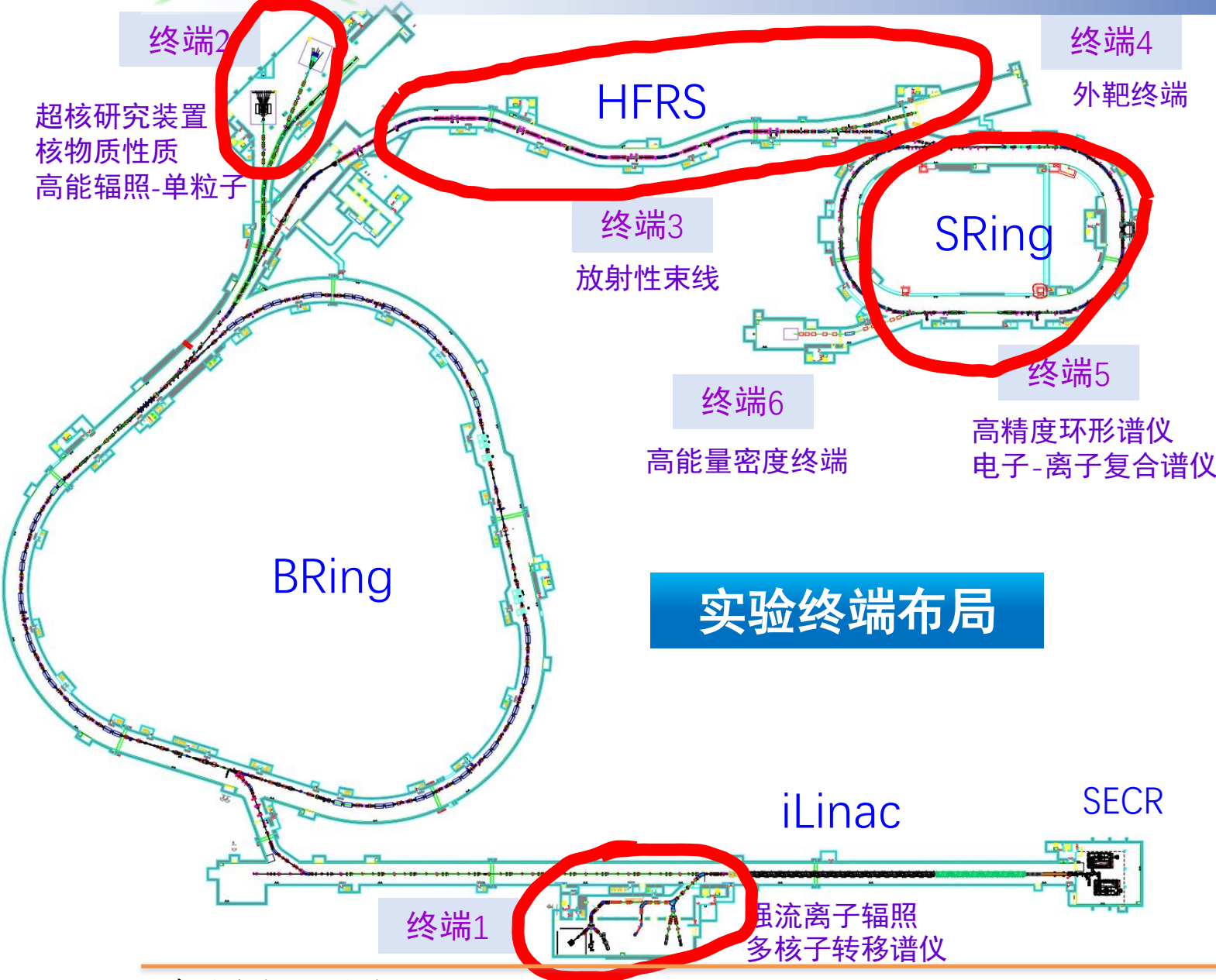
HIAF 目标

提供最高流强的重离子束流

AGS booster	BNL	5×10^9	Au^{31+}	
LEIR	CERN	1×10^9	Pb^{54+}	
SIS18	GSI	1.5×10^{11}	U^{28+}	2.7 Hz
SIS100	GSI	6×10^{11}	U^{28+}	<1 Hz
NICA	JINR	4×10^9	Au^{32+}	
HIAF	IMP	2×10^{11}	U^{35+}	3-10 Hz

面临的技术挑战：

- 第4th代ECR离子源，超导直线加速器；
- 新的束流注入方法以提高注入效率，突破空间电荷极限；
- 快的循环速度(12T/s)以减小电离束流损失和动态真空效应；

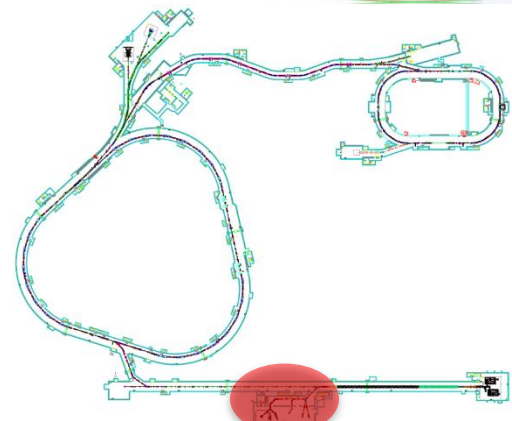


主要目标（核物理）

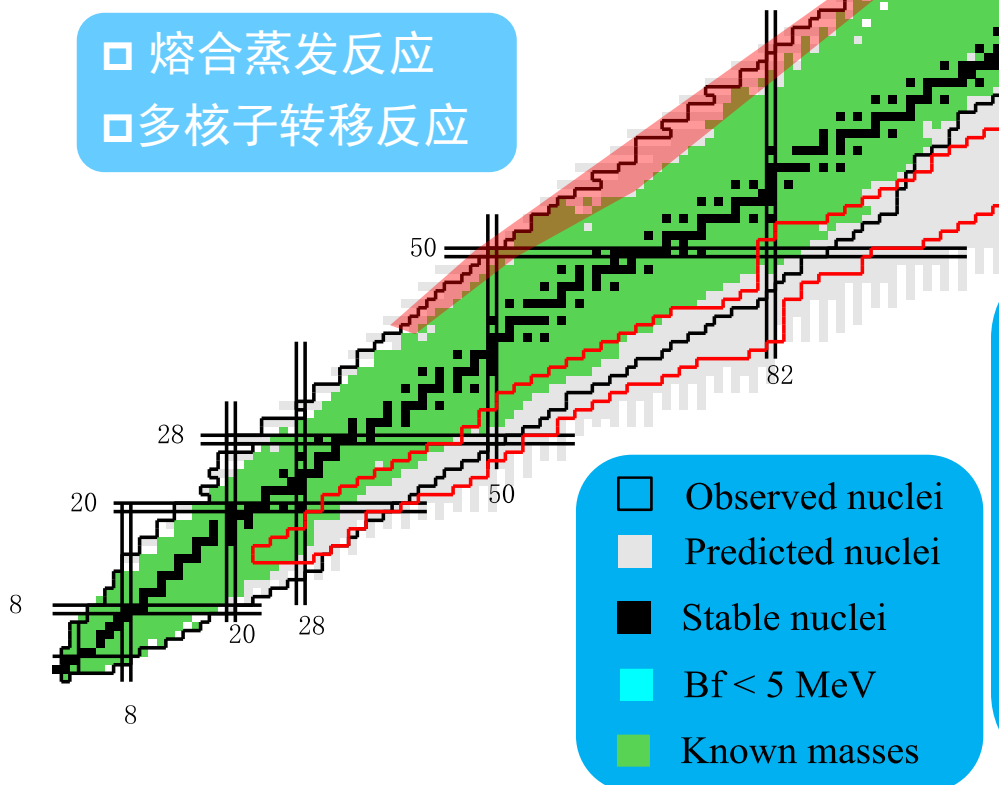
- 探索核图中迄今未知的领域
- 发现奇异的核特性，并认识其背后的物理原理
- 理解宇宙中化学元素的起源
- 描述核物质的QCD相图



低能实验终端



- 熔合蒸发反应
- 多核子转移反应



Products of fusion reactions

This architectural floor plan shows a cross-section of a building. On the left, there is a large circular area with a red boundary and a green center, containing labels 114, 184, and 162. To the right of this area is a vertical column of rooms labeled L1-L3-01 through L1-L3-06. Above these rooms is a room labeled '在线设备间' (Online Equipment Room) with a height of 3.600 meters. Further right is a long corridor with rooms labeled D101, D102, D103, and D104. The plan also includes a staircase, several equipment rooms (L1-EQ-01 to L1-EQ-04), and various other rooms and hallways. Structural elements like columns and beams are indicated by black lines, and some areas are shaded in grey or blue.

Products of MNT reactions

- To synthesize new isotopes
 - To measure nuclear masses and lifetimes
 - To build the decay schemes
 - To map out the drip lines
 - To root the decay chains of the SHN
 - To build a bridge to the island of SHN
 - To simulate the *rp* and *r* processes
 - To study the evolution of shell structure

离子种类	能量 (MeV/u)	流强 (pμA)
H_2^+	48	10
$^{18}\text{O}^{6+}$	36	10
$^{78}\text{Kr}^{19+}$	30	10
$^{209}\text{Bi}^{31+}$	30	10
$^{238}\text{U}^{34+}$	17	10

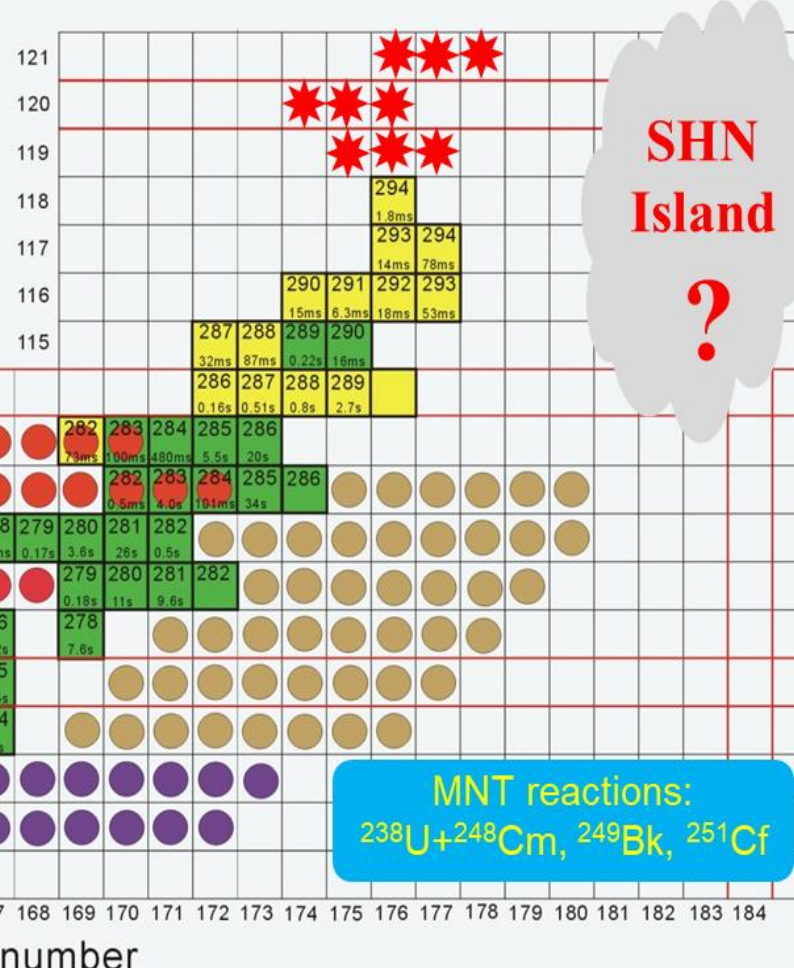
The low-energy intense beams will enable producing very n-deficient nuclei by fusion reactions and particularly heavy and super-heavy n-rich nuclei by multi-nucleon transfer reactions

Is there a limit, in terms of proton and mass numbers, to the existence of nuclei?

Unprecedented opportunities for the synthesis of new isotopes and structure studies

Proton number

Fusion reactions:



Neutron number

150 151 152 153 154 155 156 157 158 159 160 161 162 163 164 165 166 167 168 169 170 171 172 173 174 175 176 177 178 179 180 181 182 183 184

科学目标

新元素和新核素合成:

- 合成120-126号新元素
- 研究超重元素化学性质
- 合成新超重核素
-

探索超重核“稳定岛”:

- 发展直接鉴别技术和方法
- 重核间的多核子转移机制
- 合成丰中子超重核素
-

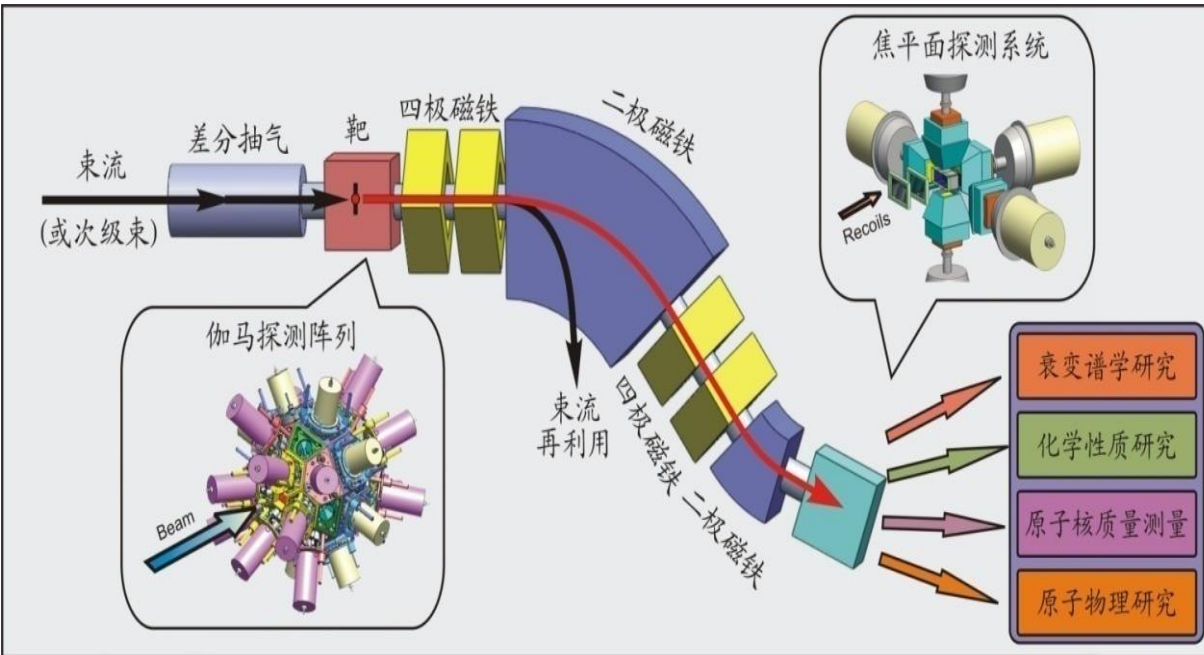
超重核素性质研究:

- 超重核素质和寿命测量
- 寻找新的K-isomers
- 超重核素中单粒子态的信息
-

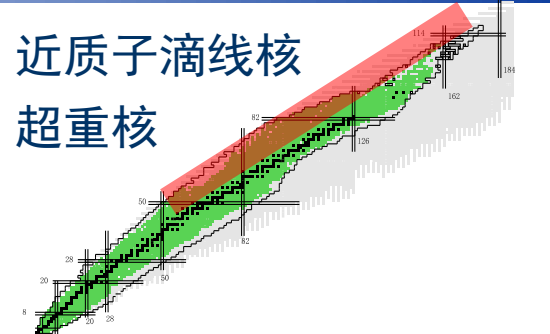
HIAF可以为新元素的研究提供最好的实验条件



低能核结构谱仪-充气反冲核分离器



近质子滴线核
超重核



谱仪性能:

- 分离传输效率>50%
- 1.0 MeV的 γ 射线:
探测效率~10%
能量分辨~2.0 keV
- 10.0 MeV的 α 粒子:
探测效率~80%
能量分辨~1.0%

超导直线加速器能够提供国际上最强的中低能重离子束流

重离子熔合蒸发反应

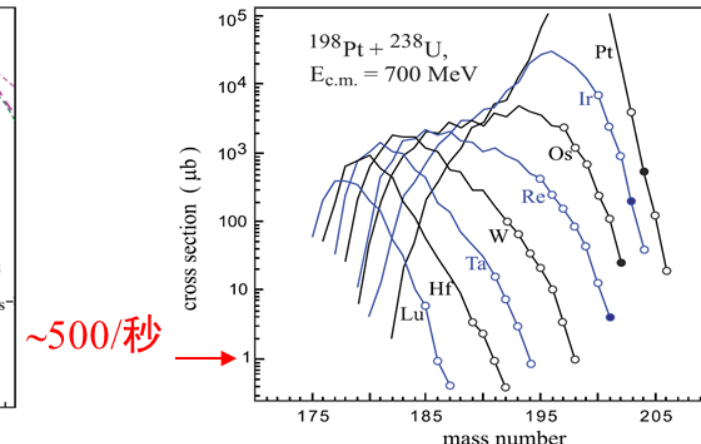
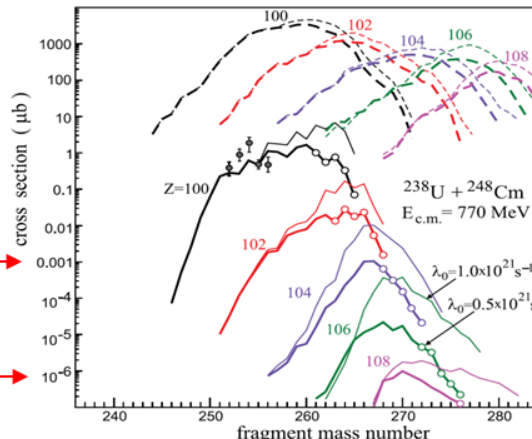
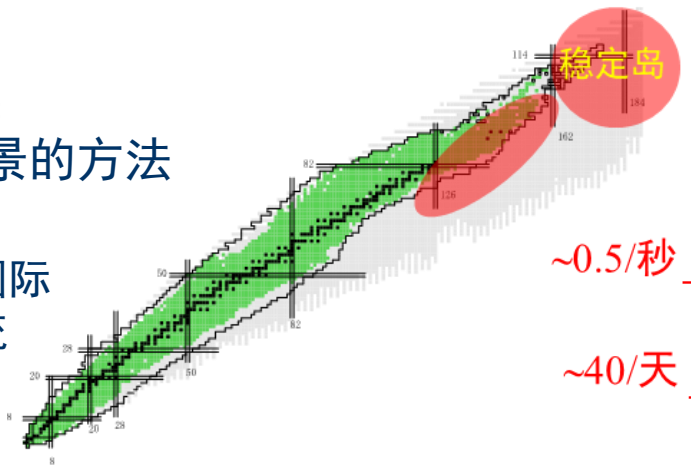
合成超重新元素（核素）、质子滴线核素；超重元素化学性质研究；探索产生超重核的反应机制；建立远离稳定线原子核在束和衰变纲图

Separation and Identification of Products from Multi Nucleon Transfer(MNT) Reactions

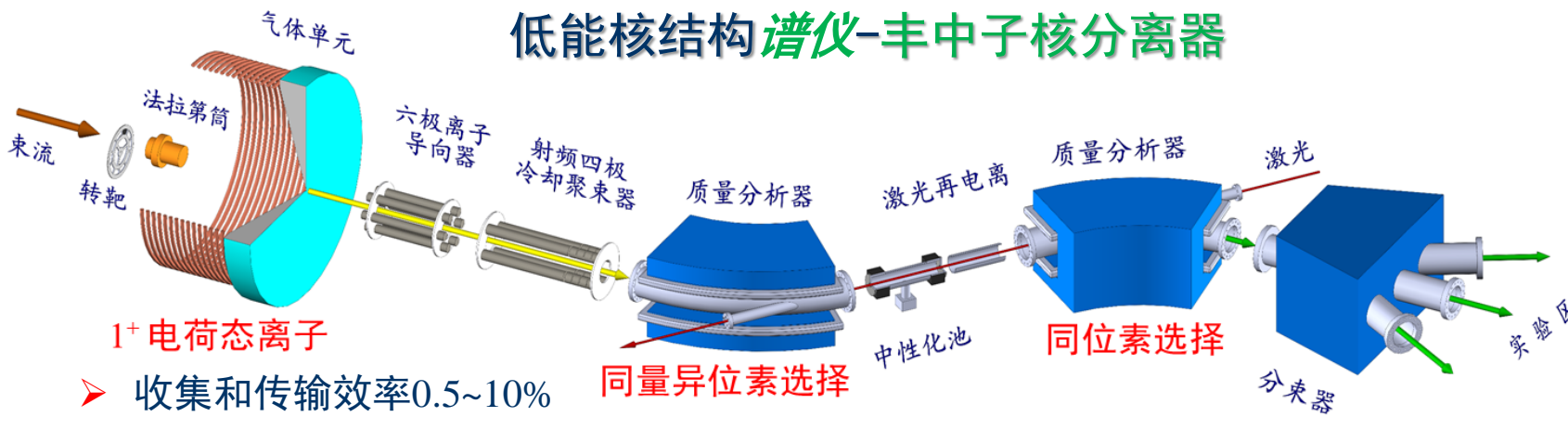
重核间多核子转移反应：
产生丰中子重核最有前景的方法

超导直线加速器能够提供国际上最强的中低能重离子束流

将形成在国际上独具特色、极具竞争力的丰中子重核素和超重核素合成及其衰变性质研究、超重元素化学性质研究、超重原子结构研究综合实验平台



低能核结构谱仪-丰中子核分离器



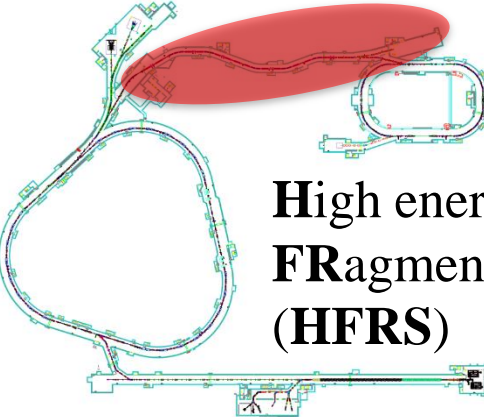
- 原子核衰变测量装置：研究原子核衰变性质和结构
- 多反射飞行时间谱仪：精确测量原子核质量
- 彭宁离子阱：精确测量原子核质量
- 共线激光谱仪：测量原子核电荷分布半径等
- 气相和液相热色谱仪：研究超重元素化学性质

产生和制备低能、高品质、脉冲化丰中子重核和超重核束流

放射性束线



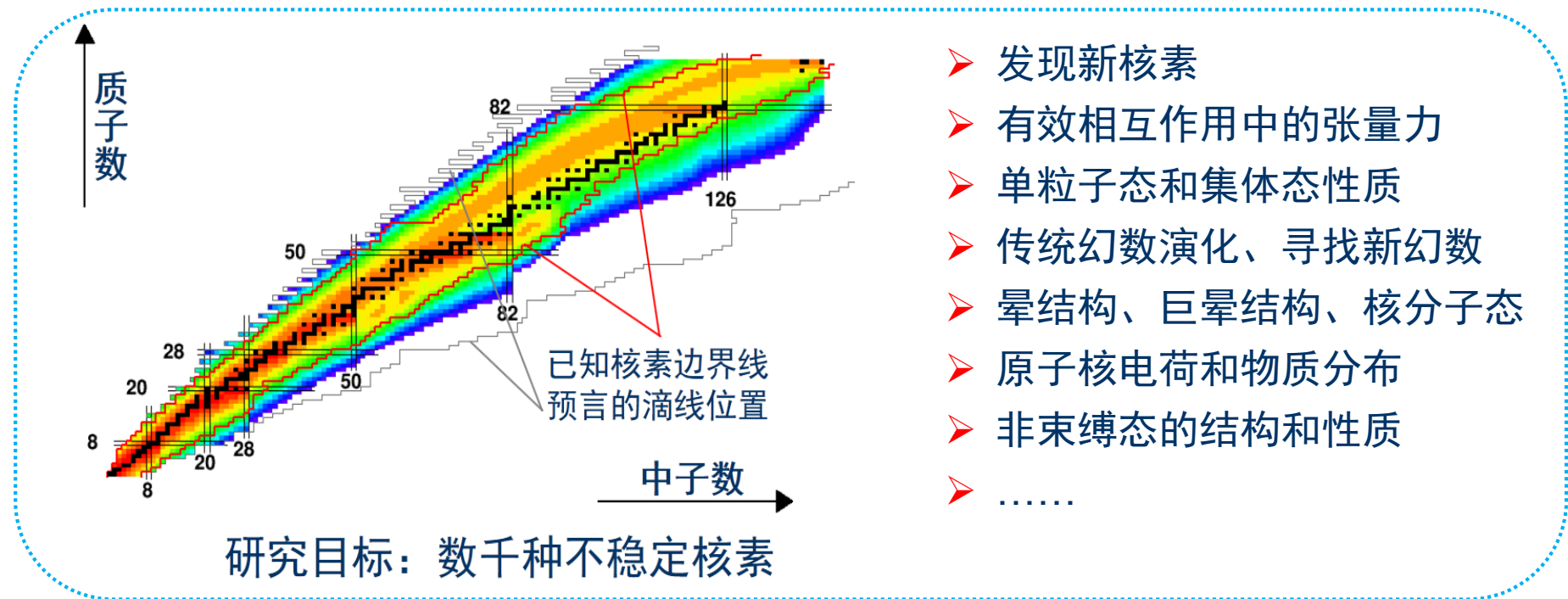
To explore the hitherto unknown territories and find new phenomena



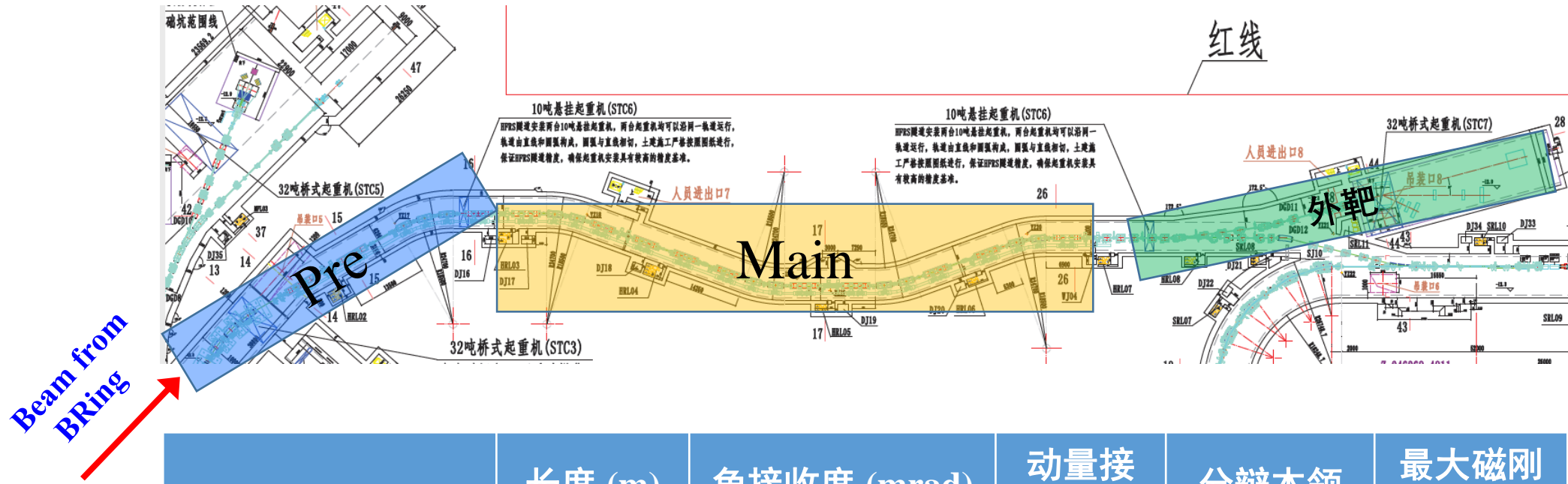
High energy
FRagment Separator
(HFRS)

- 通过弹核碎裂及重核的飞行中裂变产生RIBs
- Pre/Main结构：去除强流主束、**具备多种工作模式**
- 超导磁铁：更大接收度，**更高磁刚度**，拓展研究领域

- 原子核存在的极限是什么（特别是对丰中子核）？
- 远离稳定线的核物质有什么新的形态？
- 在极丰中子区域量子能级是如何演变的？
- 远离稳定线的集体运动有什么新的形式？
- 奇特核中动力学对称性是如何体现的（特别是沿着N=Z线）？
- ...

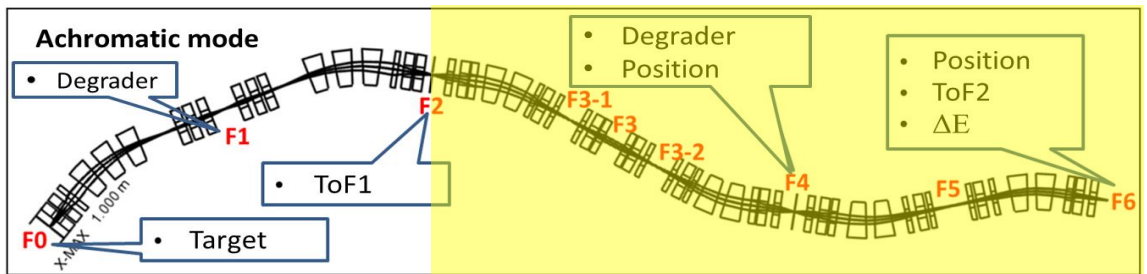


- 发现新核素
- 有效相互作用中的张量力
- 单粒子态和集体态性质
- 传统幻数演化、寻找新幻数
- 晕结构、巨晕结构、核分子态
- 原子核电荷和物质分布
- 非束缚态的结构和性质
-

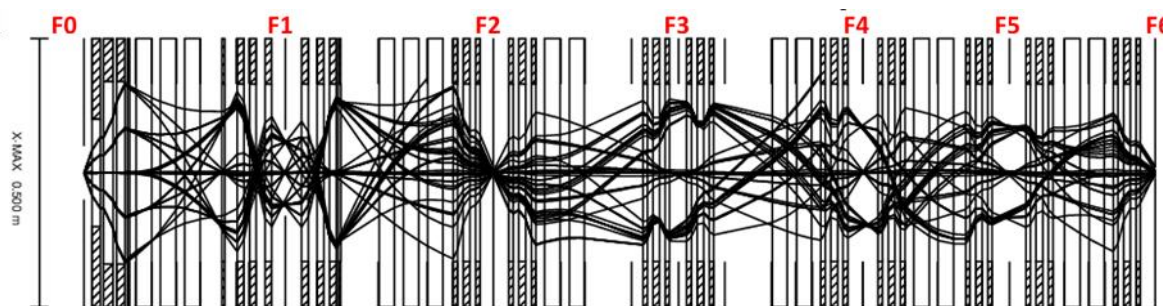


	长度 (m)	角接收度 (mrad)	动量接收度 (%)	分辨本领	最大磁刚度 (Tm)
HFRS NIM.B 469(2020),1	191.8	±30 (X); ±15 (Y)	±2.0	850/1100 (ΔX=±1mm)	25
SuperFRS NIM.B 204(2003),71	182.2	±40 (X); ±20 (Y)	±2.5	750/1500 (ΔX=±1mm)	20
BigRIPS Prog.Theor.EXP.Phys.2012,03C003	78.2	±40 (X); ±50 (Y)	±3	1260/3420 (ΔX=±1mm)	9.5
ARIS NIM.B 317(2013)349	86.8	±40 (X); ±40 (Y)	±5	1720/3000 (ΔX=±1mm)	8

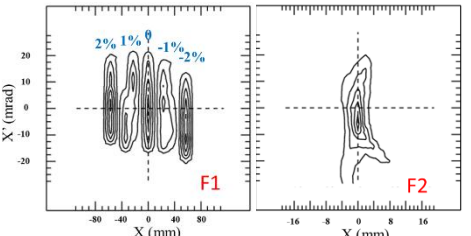
Achromatic mode



F2->F6: 117m

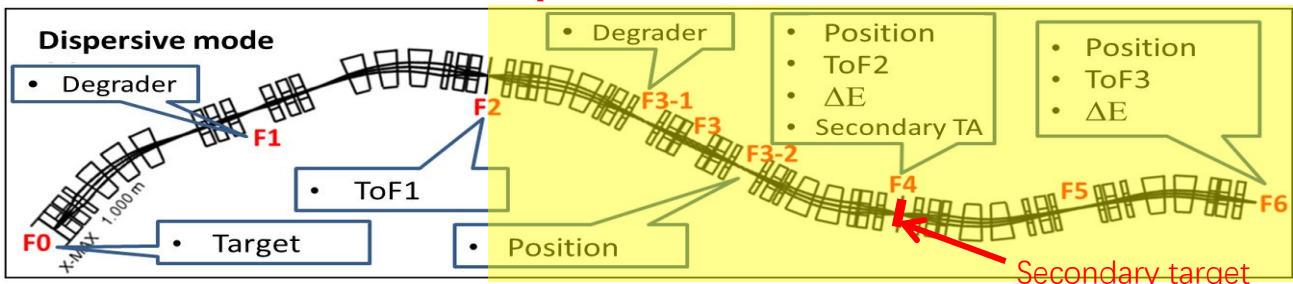


$$\begin{aligned}\Delta X &= \pm 1\text{mm} \\ \Delta X' &= \pm 30\text{mrad} \\ \Delta Y &= \pm 1.5\text{mm} \\ \Delta Y' &= \pm 25\text{mrad} \\ \Delta P/P &= \pm 2\% \end{aligned}$$

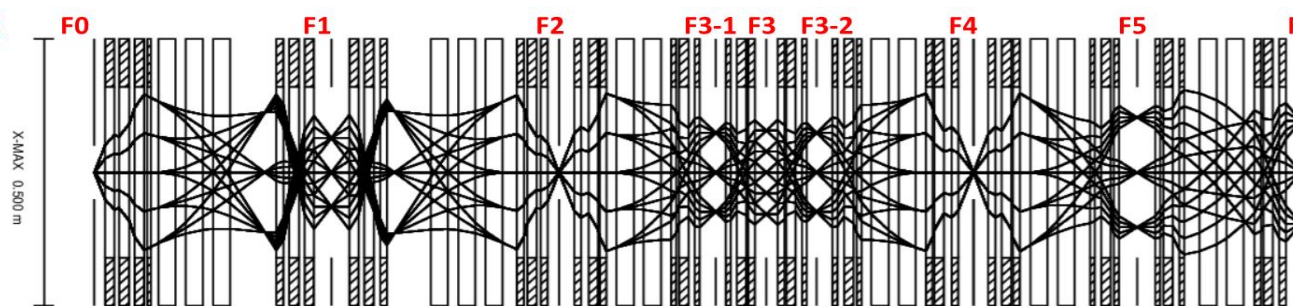


分辨本领	最大磁刚度 (Tm)
F1:850; F4:1100	25

Dispersive mode

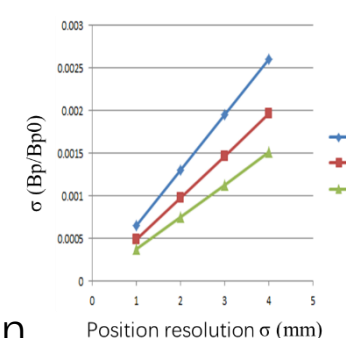


F2->F4: 65m



Fragment Separator + Zero Degree Spectrometer

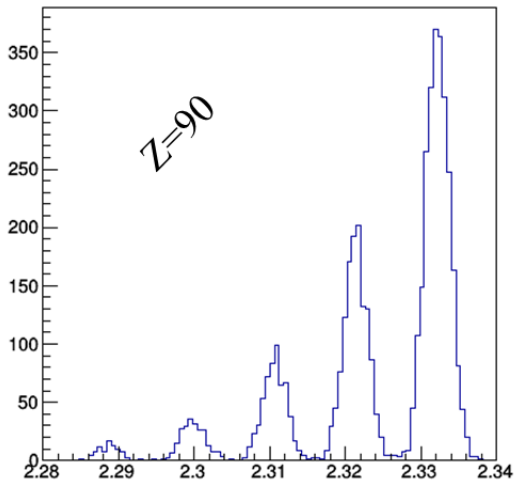
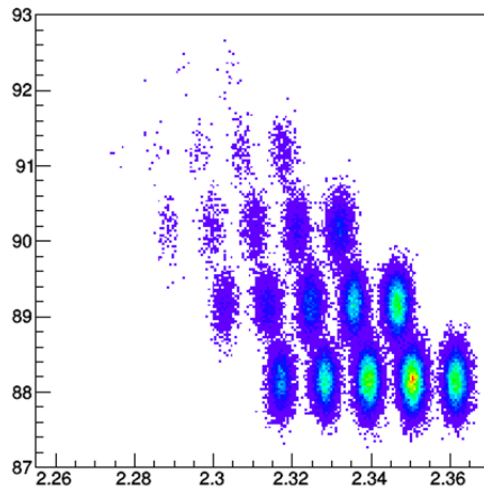
分辨本领	最大磁刚度 (Tm)
F1:850; F3-1:700	25
F6:1000	25



Detectors aided high mass resolution

Achromatic mode

^{238}U @800AMeV + ^{12}C -> ^{208}Th
 $B\rho = 10.66\text{Tm}$

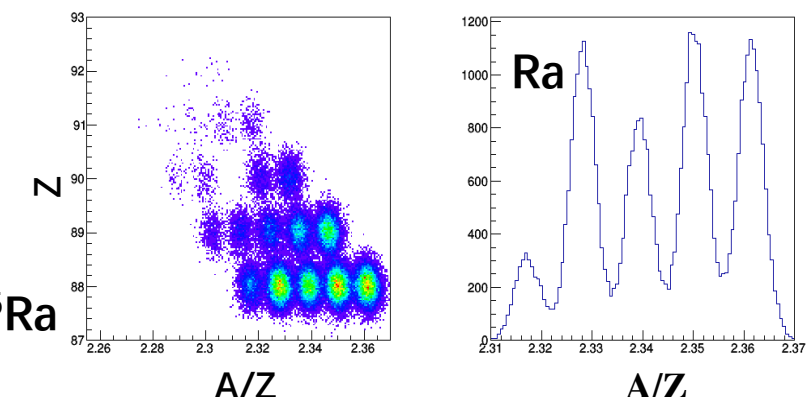
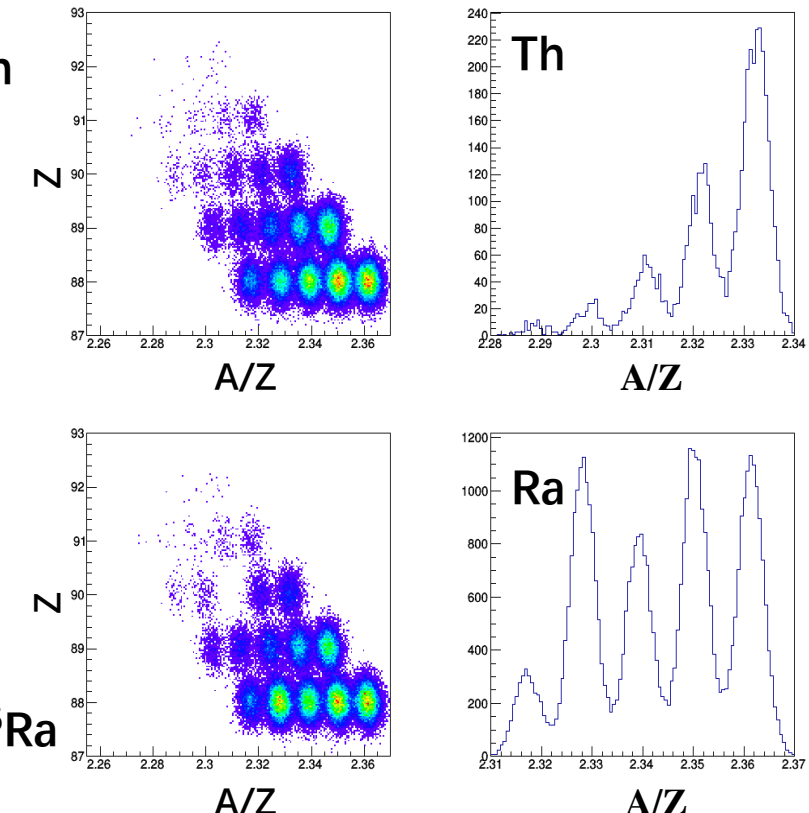


F0 – F4:
 $^{238}\text{U} + ^{12}\text{C} \rightarrow ^{208}\text{Th}$
800AMeV
 $B\rho = 10.66\text{Tm}$



F4 – F6:
 $^{208}\text{Th} + ^{12}\text{C} \rightarrow ^{205}\text{Ra}$
 $B\rho = 10.22\text{Tm}$

Dispersive mode



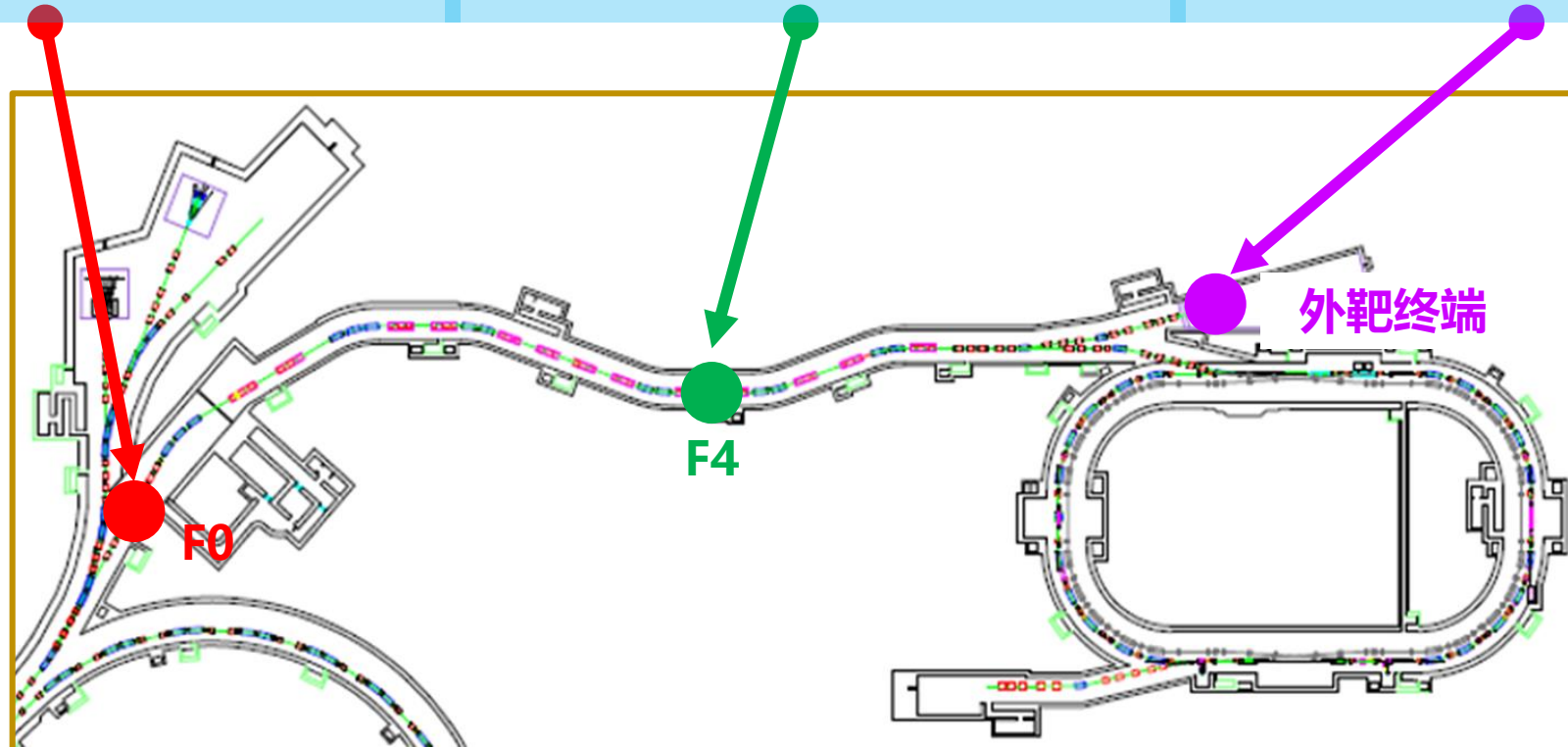
- ✓ Time resolution (σ) : 50ps
- ✓ Position resolution (σ) : 1.0mm
- ✓ Energy resolution (σ) : 0.5%

F0初级靶实验

F4次级靶实验

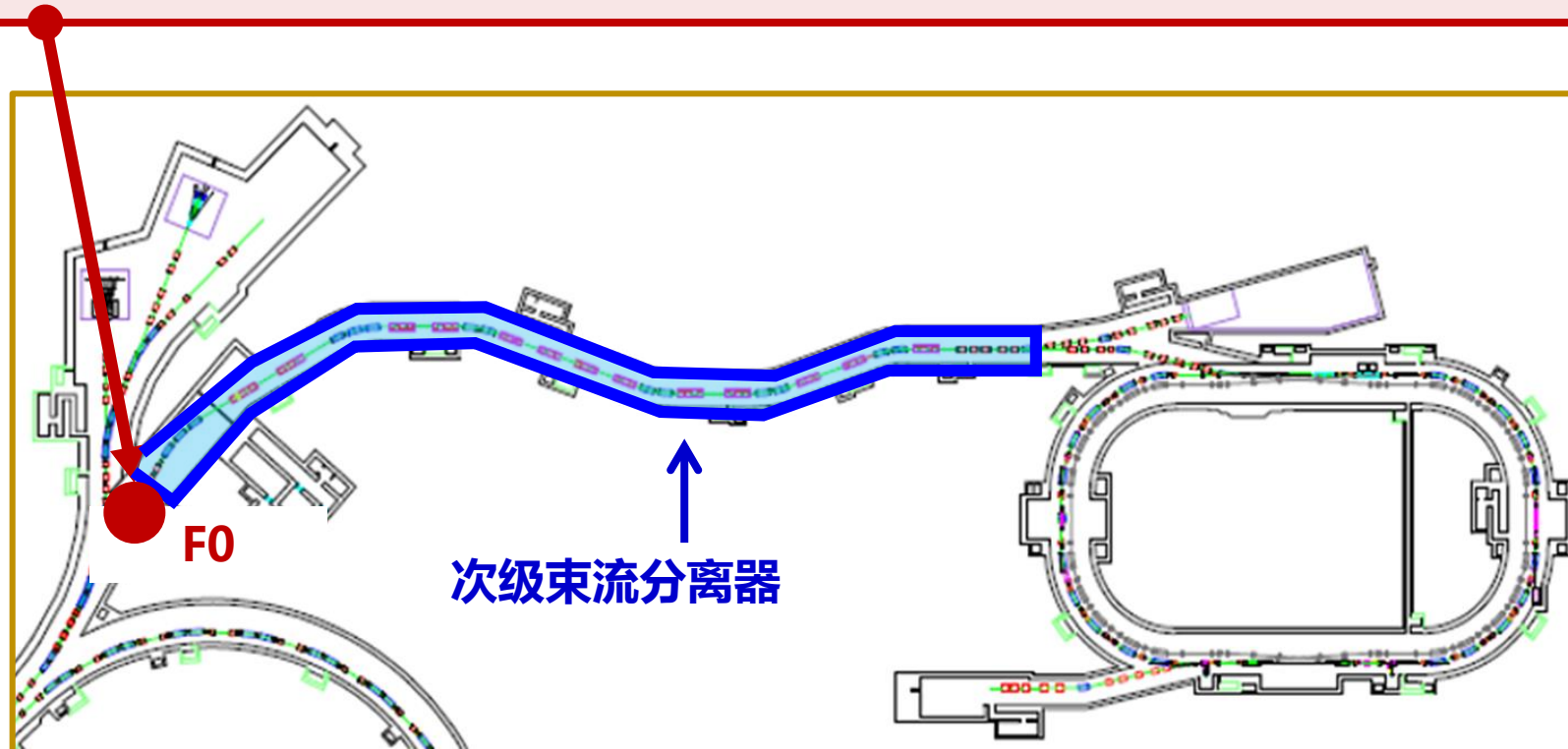
外靶终端实验

HFRS上可开展物理实验的区域



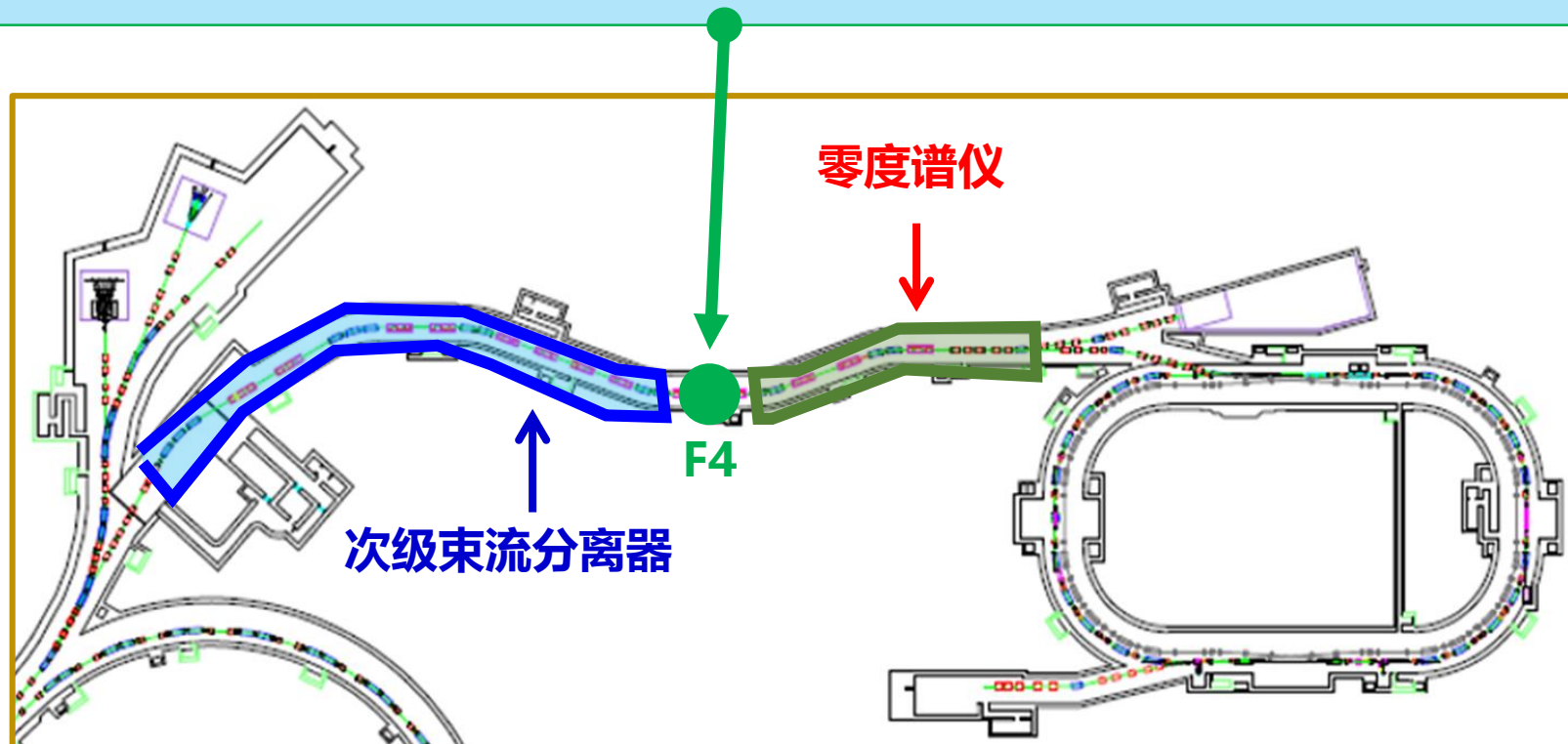
基于HFRS的碎片分离束线功能，结合束线探测器可开展的实验研究：

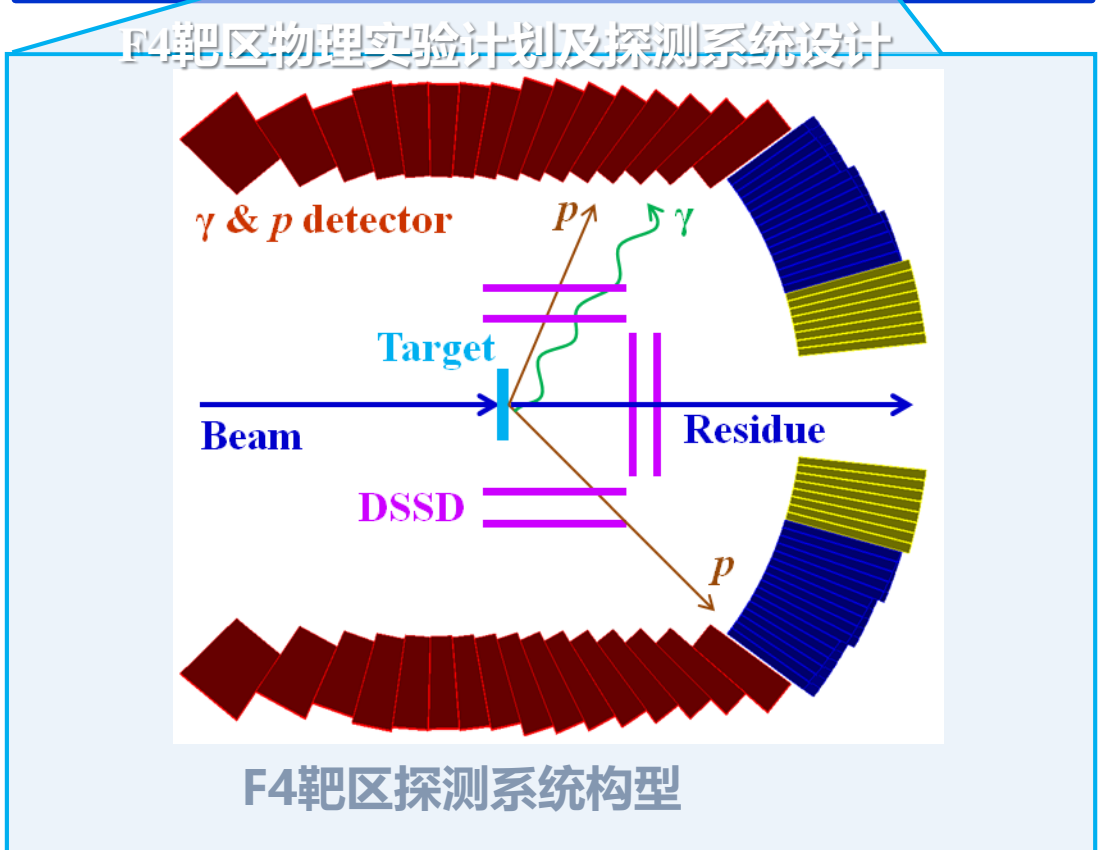
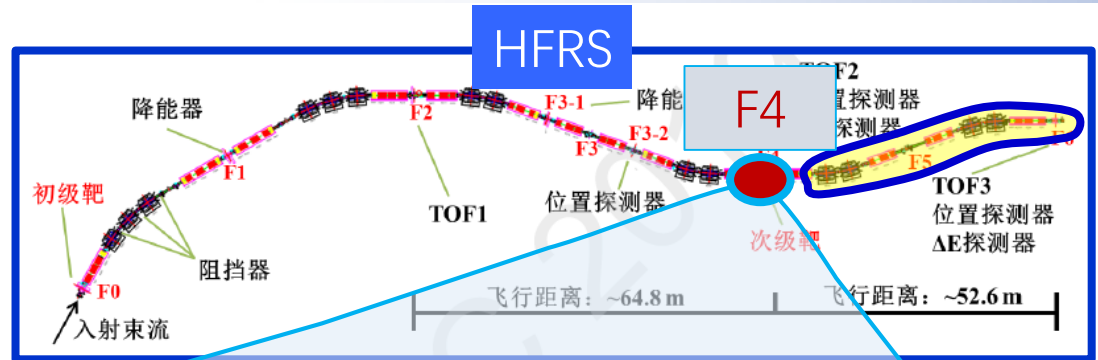
- RIB production mechanism
- Discovery of new isotope
- Mass measurement of extremely short-lived nuclei
- Mechanism of fission/spallation
-



利用HFRS的F0-F4部分作为碎片分离束线及F4-F6作为零度谱仪，
结合新建造的探测装置，可开展多种类型的物理实验：

- Interaction cross section → nuclear radii and matter distribution, halo and skin structures
- Knockout/Quasifree knockout → single-particle structures, unbound states/nuclei, clusters
- Charge change/exchange → Gamow-Teller strength, spin-dipole resonance, neutron skins
-





- New magic numbers ● Shell evolution
- Shape coexistence ● halos

② F4-F6谱仪: 类弹产物测量

- Interaction cross section/Fragmentation cross section
- Knockout (inclusive cross section + momentum distr.)
- Charge exchange
-

② CsI阵列: 在束 γ 谱测量

- Spectroscopy of nuclei at limits $\rightarrow E(2^+), E(4^+), \dots$
- Knockout (exclusive cross section + momentum distr.)
- Inelastic/Coulomb excitation $\rightarrow B(E2)$
-

② CsI阵列+DSSD阵列: 轻带电粒子 $\Delta E, E$, 径迹

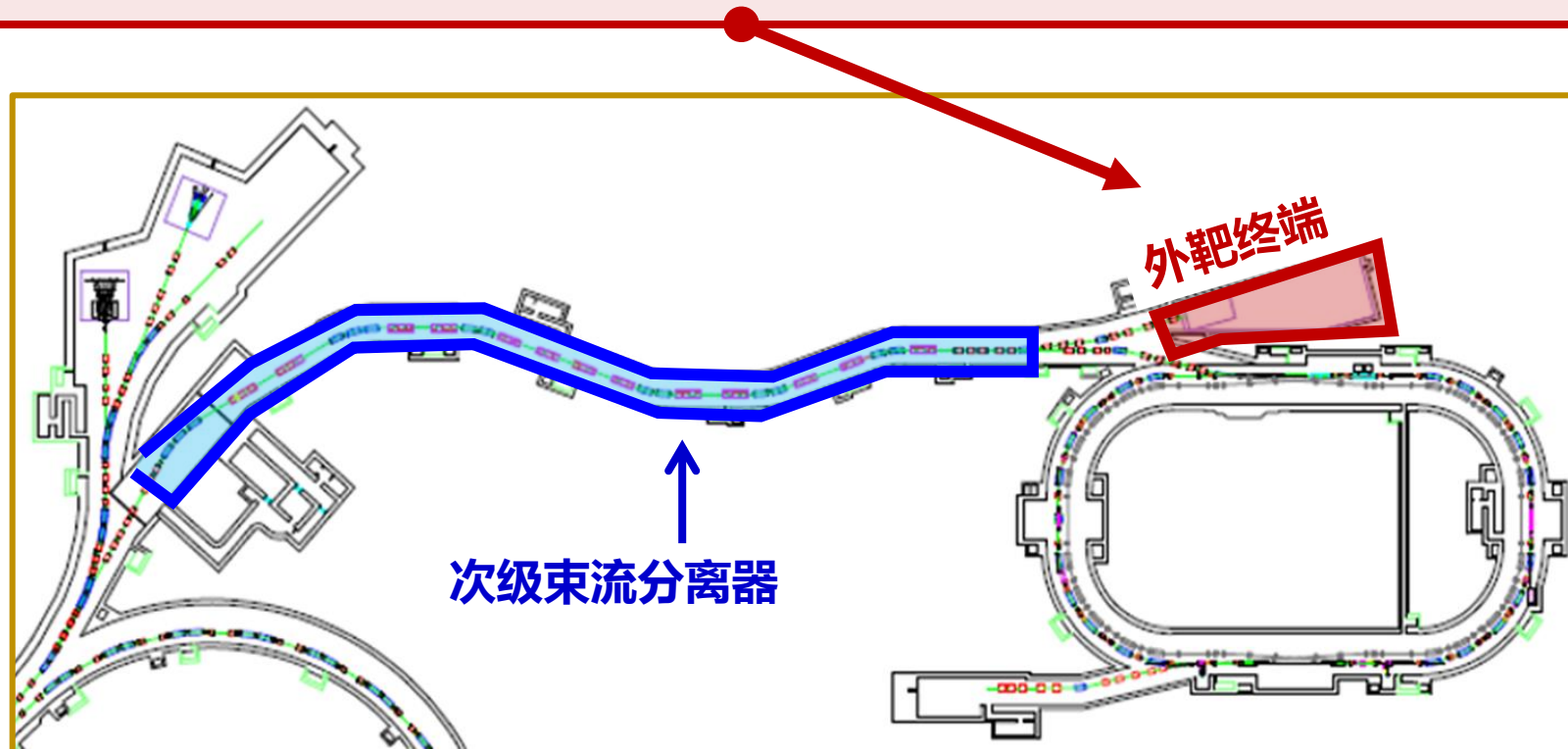
- Quasi-free scattering
- Missing mass \rightarrow unbound states
- Reaction mechanism of knockout/quasi-free/...
-

外靶终端区域预留空间充足（面积~400 m²），
将来可建造多种实验装置、开展多种类型的物理实验

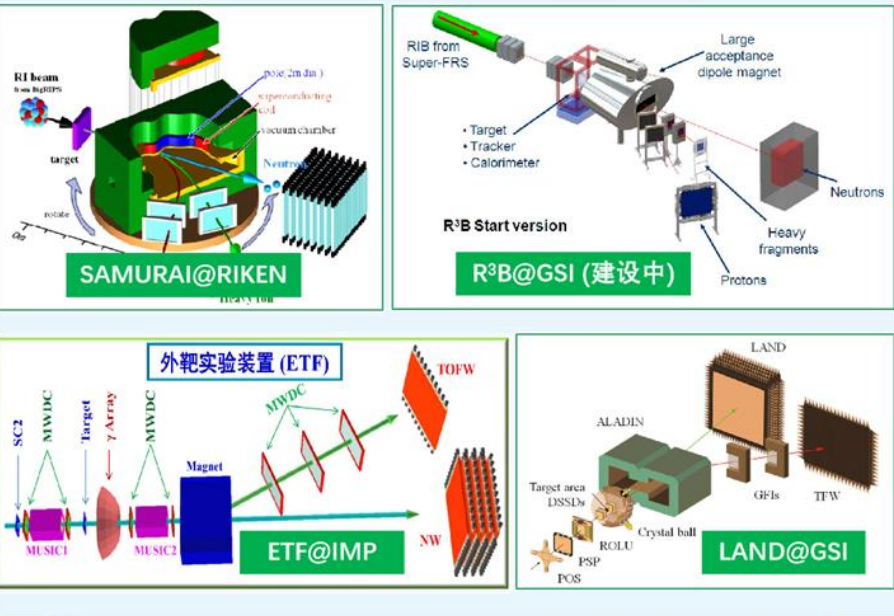
大接收度谱仪装置
(高能放射性束反应实验)

束流慢化+低能实验装置
(低能放射性束反应实验)

束流阻停+衰变实验装置
(衰变实验)



大接收度磁谱仪



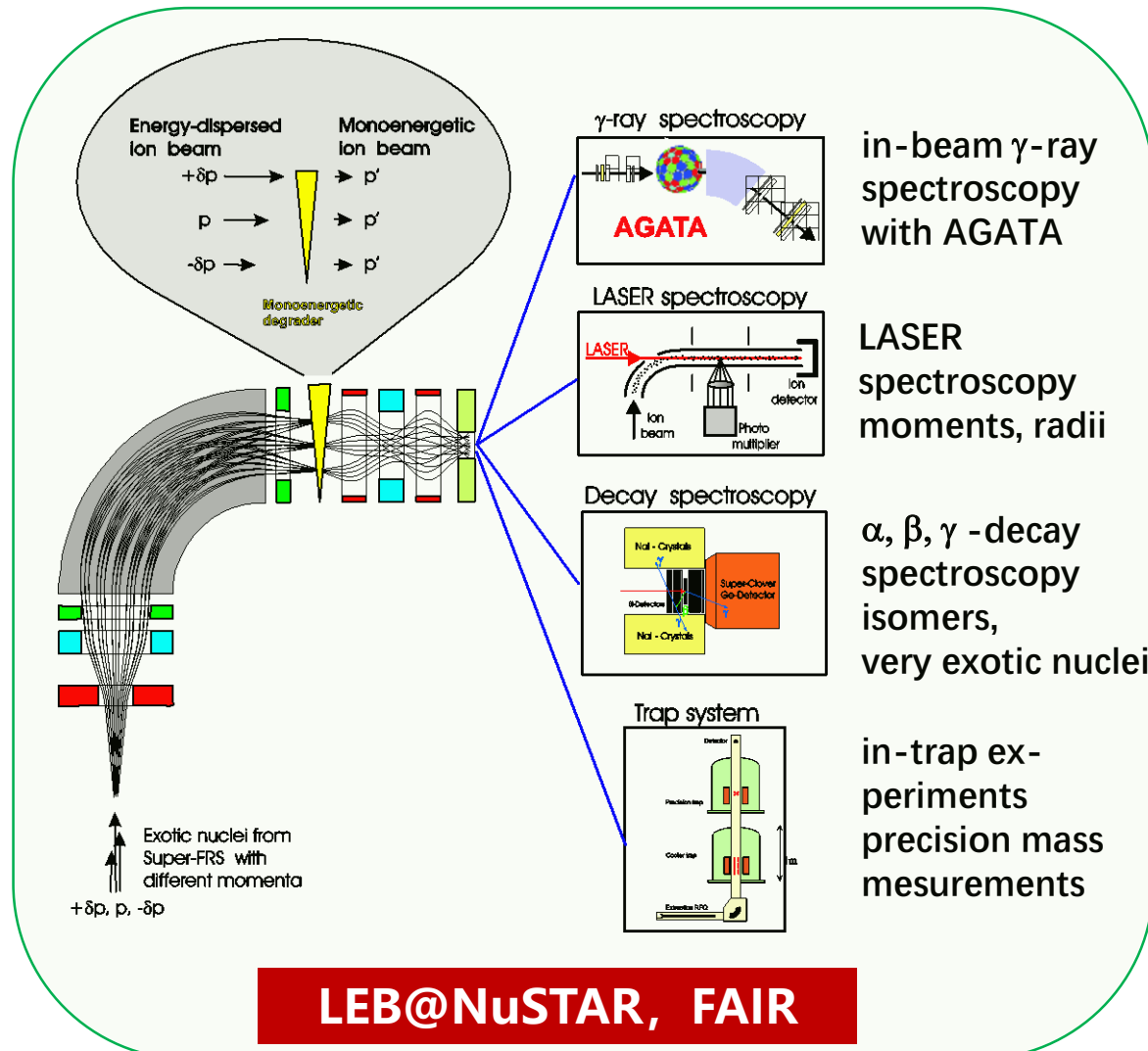
实验探测及物理研究主要目标:

全粒子测量 (运动学完全测量)

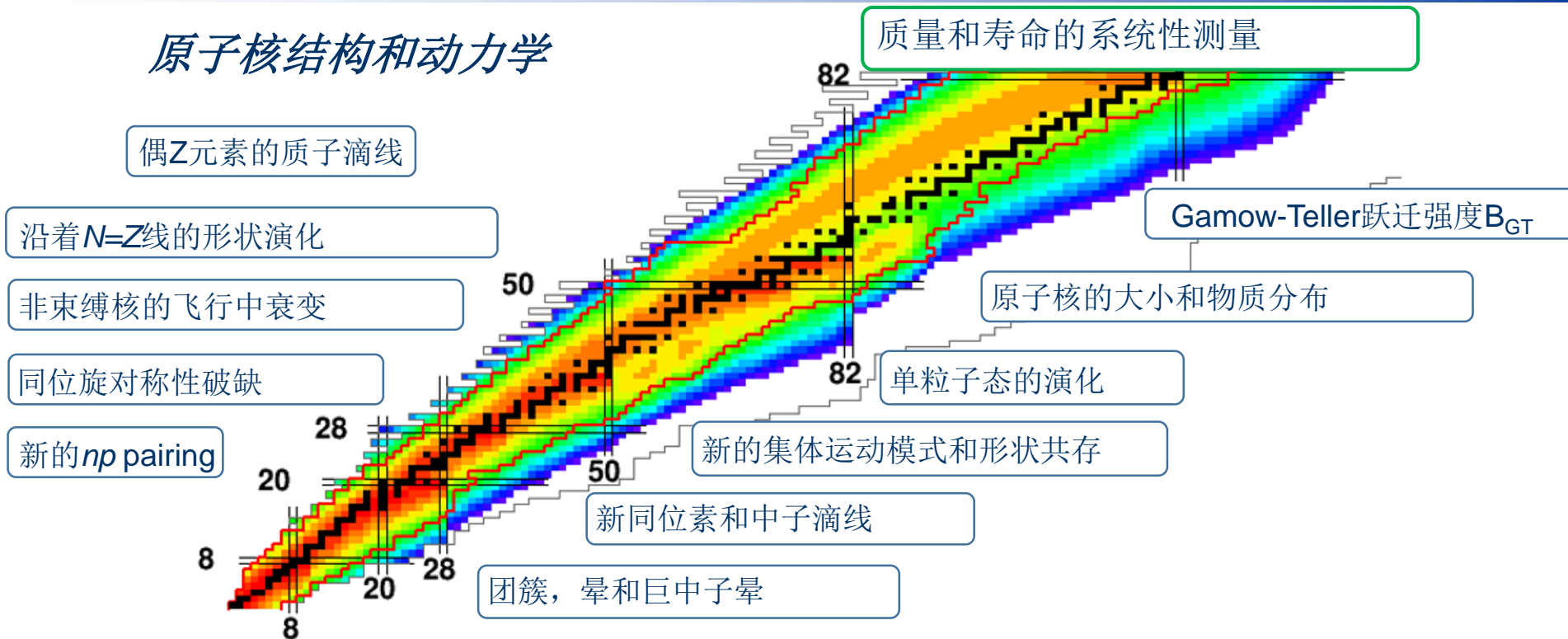
Invariant Mass Measurement
Missing Mass Measurement

Nuclear structure and dynamics of
unbound states/nuclei

放射性束的慢化和阻停



原子核结构和动力学



Experimental methods

- interaction cross section/elastic scattering →
- knockout/quasi-free knockout →
- electromagnetic excitation →
- charge-exchange reactions →
- fission →
- spallation →
- fragmentation/cascade fragmentation →
- slowed/stopped beam experiment →

Physics goals

nuclear radii and matter distribution, halo and skin structures
 single-particle structures, unbound states/nuclei, clusters
 $B(E2)$, pigmy/giant resonance, astrophysical S factor
 Gamow-Teller strength, spin-dipole resonance, neutron skins
 shell structure, dynamical properties
 reaction mechanism, applications (waste transmutation, ...)
 new isotope, mass of very exotic nuclei, γ -ray spectroscopy, equation of state
 low energy experiment, β delayed γ , p, n, ... emission, isomer decay, proton decay

Nucleon distributions or radii

Total interaction cross sections

Elastic proton scattering

Proton distributions or radii

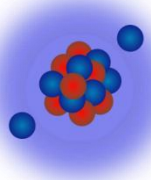
Isotope shifts

Electron scattering

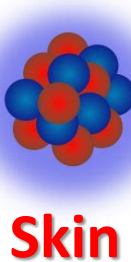
μ atom

Charge changing cross sections

Halo



- Halos in heavier nuclides
- Giant neutron halos with > two neutrons
- Deformed halos
- Coupling of continuum and discrete states



Skin

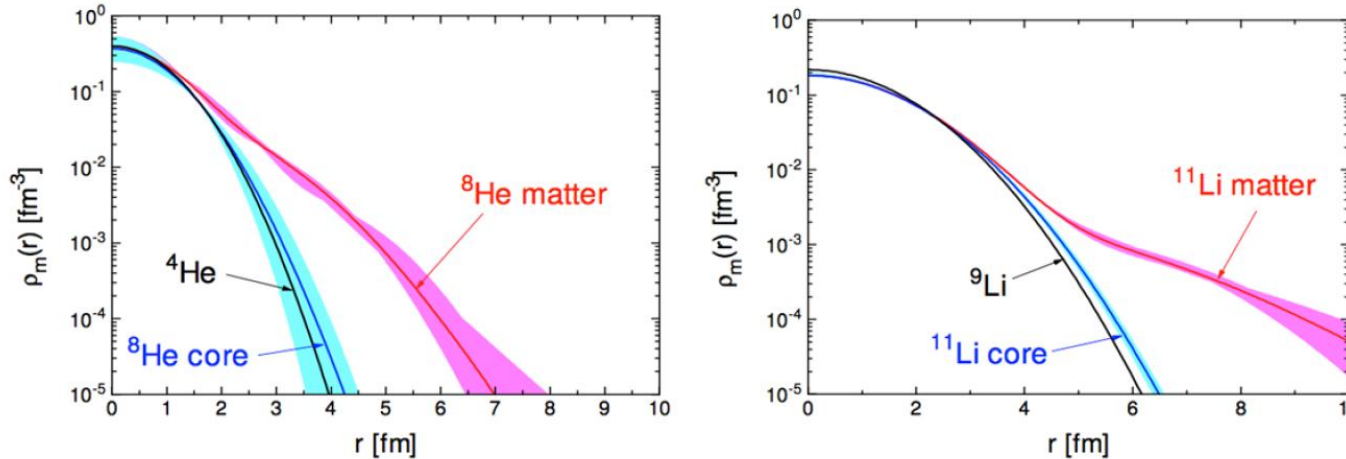
Neutron distributions or radii

- Nuclear size evolution of n-rich nuclides
- New shell closures in n-rich regions
- Constrains on nuclear theories
- EOS for cold asymmetric nuclear matter

Measurements of nuclear matter and/or charge radii provide the most original evidences for neutron and proton halos, neutron skins, and new magic numbers

Proton scattering or light particle scattering with low-momentum transfer provides crucial information on nuclear matter distribution and incompressibility of nuclide

Pilot IKAR experiments performed at FRS.

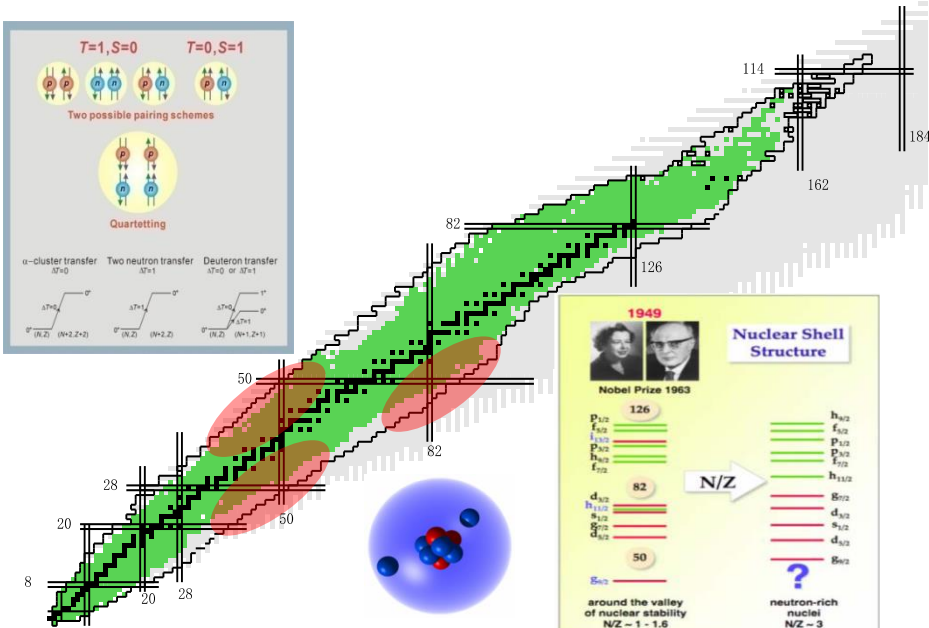
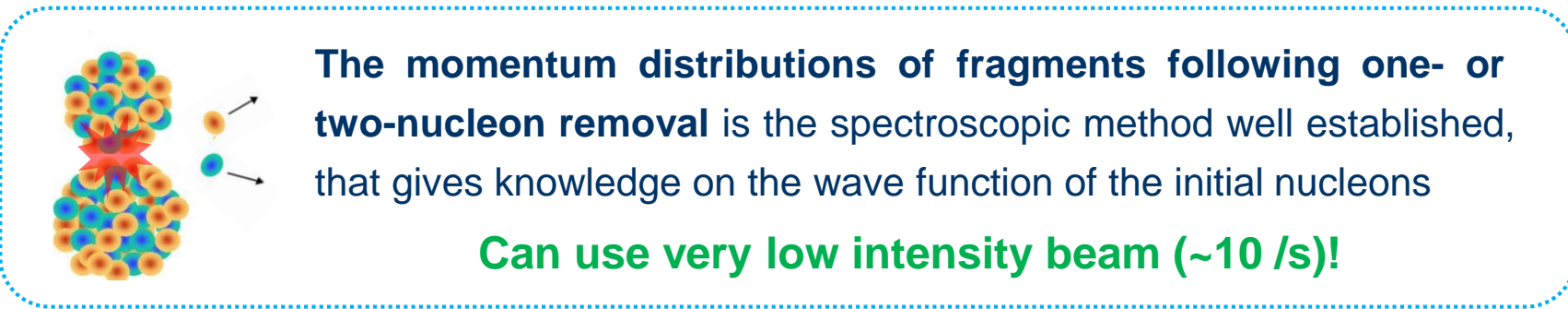


In inverse kinematic reactions using an active target, precisely measure the angular distribution in a broad angular region including the first diffraction minimum

In the center-of-mass frame, proton wavelength of ~ 1 fm at an incident energy of 500 MeV/u

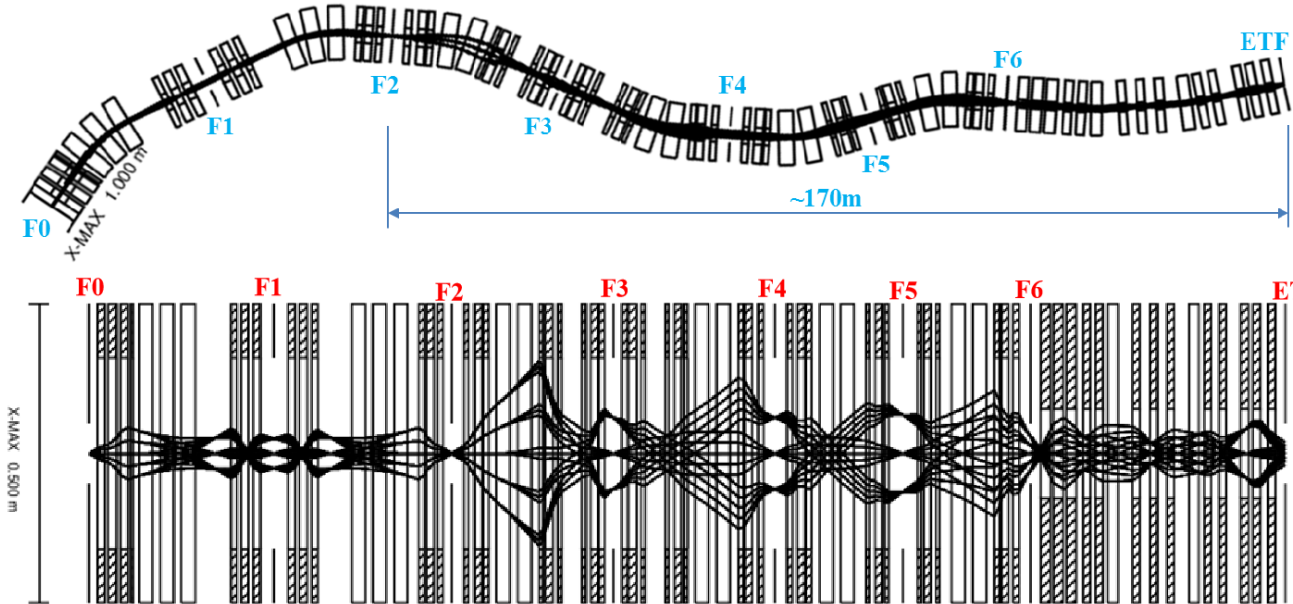
- Measurements of the nucleon density distribution by elastic proton scattering
- Study of the N/Z ratio dependence of the saturation density; the nuclear density near the maximum of $r^2\rho(r)$ sensitive to the saturation density of nuclear matter

In order to understand the properties of nuclides far away from the stability, it is crucial to precisely locate the position of single particle states near the Fermi surface, and to investigate the degree to which their wave functions reflect pure single-particle motion



Systematic study along isotopic and/or isotonic chains:

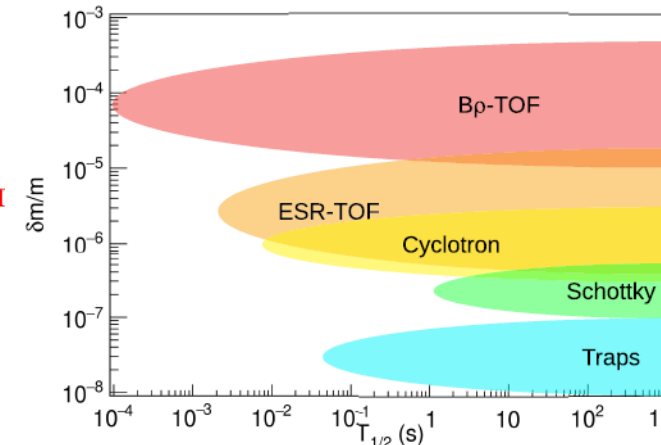
- Evolution of single particle states?
- Robustness of the shell closures?
- $T=0, S=1$ proton-neutron pairing?
- Coupling to the continuum?
- Heavier Halos and giant halos?
-



$$\left(\frac{\sigma_{m_0}}{m_0}\right)^2 = \left(\gamma^2 \frac{\sigma_\beta}{\beta}\right)^2 + \left(\frac{\sigma_P}{P}\right)^2 = \left[1 - \left(\frac{L}{ct}\right)^2\right]^{-2} \left(\frac{\sigma_t^2}{t^2} + \frac{\sigma_L^2}{L^2}\right) + \frac{\sigma_P^2}{P^2}$$

	E (MeV/u)	v (cm/ns)	L (m)	tof (ns)	σ_{tof} (ns)	$\sigma_{\text{tof/tof}}$	D (mm)	σ_R (mm)	σ_R/D	σ_m/m
SPEG	100	12.8761	82	636.8388	0.085	1.33E-04	10000	1	1.00E-04	1.92E-04
S800	100	12.8761	59	458.2133	0.08	1.75E-04	11000	0.25	2.27E-05	2.15E-04
SHARAQ	300	19.6094	105	535.4575	0.017	3.17E-05	14760	0.127	8.60E-06	5.62E-05
HFRS	400	21.4216	170	793.5915	0.03	3.78E-05	12000	0.3	2.50E-05	8.12E-05

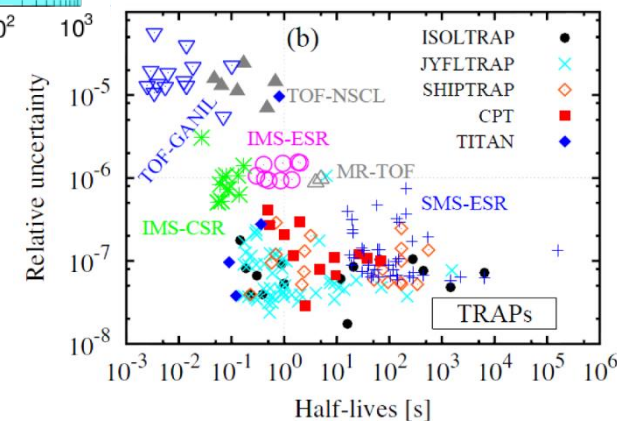
飞行时间法测量原子核质量(B β -TOF mass measurement)



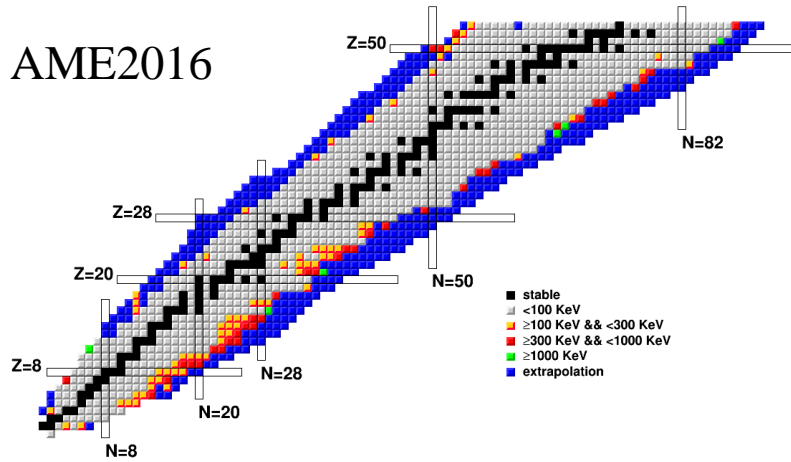
International Journal of Modern Physics E 28(04), 1930005 (2019)

2003年-2016年间首次测
量质量的原子核

EPJ Web of Conferences 109, 04008 (2016)



AME2016



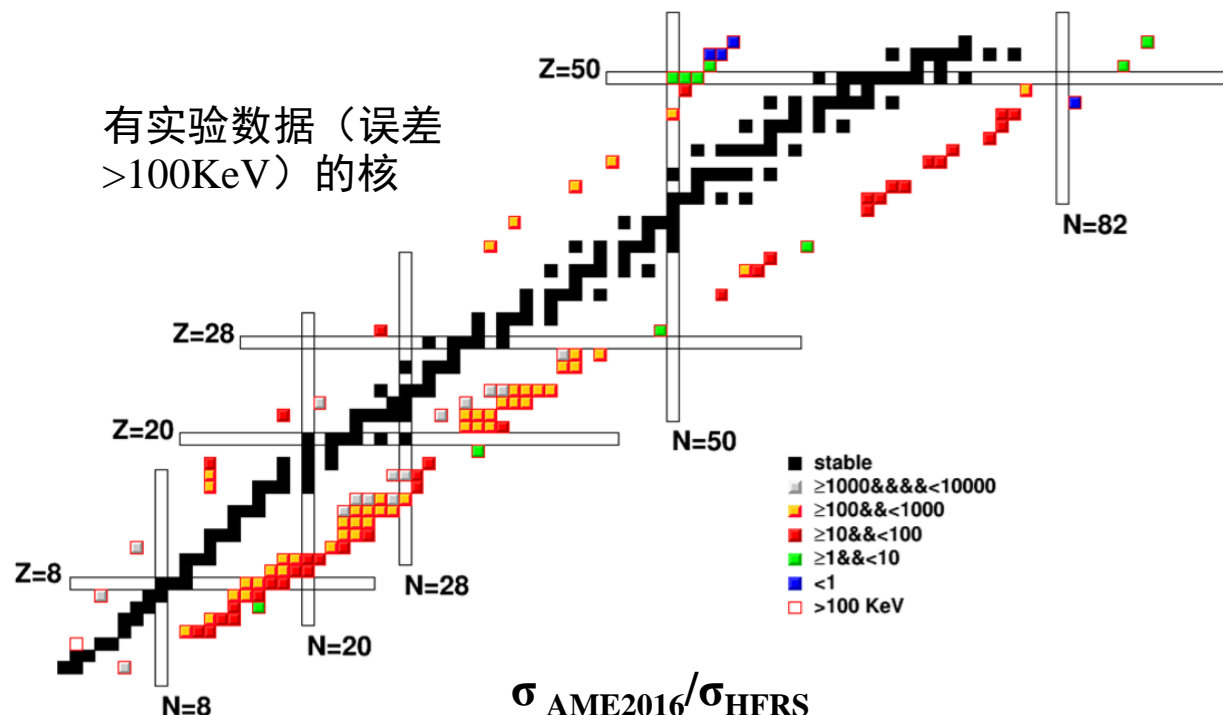
$$\sigma_m/m = 8.12 \times 10^{-5}, \text{ 则对 } A=100$$

若统计单个事件 $\sigma_m \sim \pm 3.8$ MeV;
统计50000事件: $\sigma_m \sim 34$ KeV;
统计500事件: $\sigma_m \sim 340$ KeV;

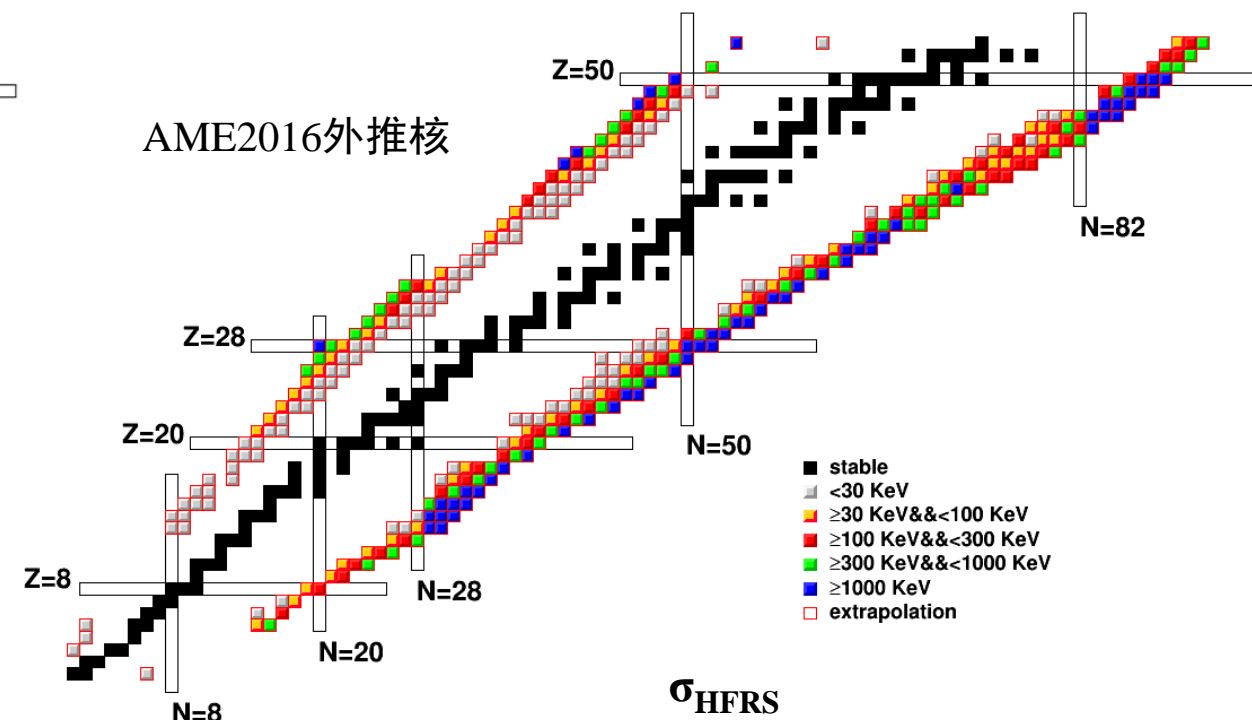
统计5000事件: $\sigma_m \sim 107$ KeV
统计50事件: $\sigma_m \sim 1074$ KeV

周期13秒，实验时间2天

有实验数据（误差
 >100 KeV）的核



AME2016外推核



The tensor forces are essential to bind nucleons together in light nuclides, but they are not treated explicitly in models such as mean field models and shell models

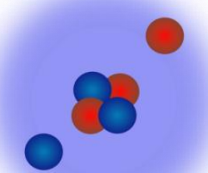
The pion interaction:

$$\vec{\sigma}_1 \cdot \vec{q} \vec{\sigma}_2 \cdot \vec{q} = \frac{1}{3} q^2 S_{12}(\hat{q}) + \frac{1}{3} \vec{\sigma}_1 \cdot \vec{\sigma}_2 q^2$$

The tensor force is as important as the central forces!

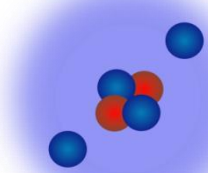
In a three-body model

${}^6\text{Li}$



$\alpha + n + p$

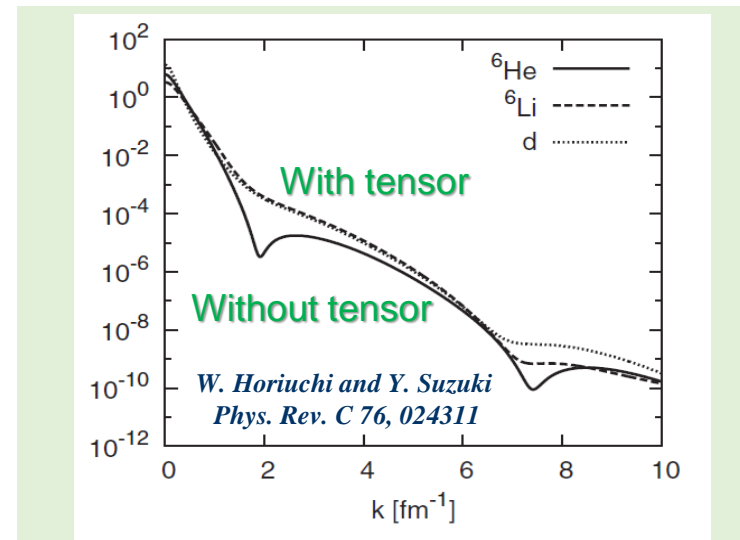
${}^6\text{He}$



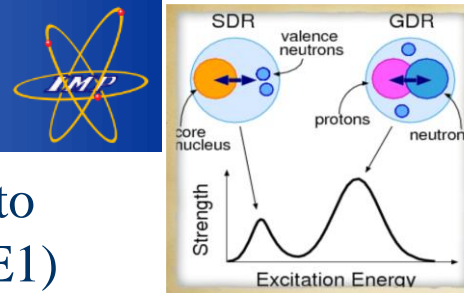
$\alpha + n + n$

The tensor force leads to a strong correlation between a np pair and high-momentum nucleons in nuclei. While the high-momentum nucleon is picked up by a particle, the correlated nucleon may be emitted and measured using (p, pd), (p, nd), and (d, pt) reactions

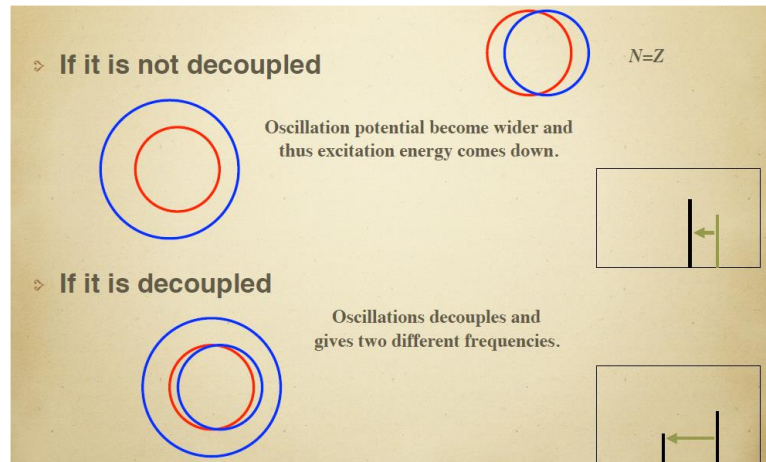
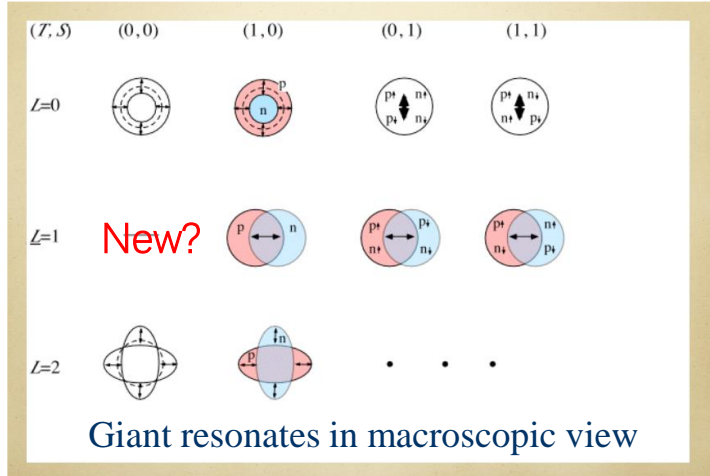
Proposed by I.Tanihata and S.Terashima



The momentum distribution of relative motion of the two nucleons in ${}^6\text{Li}$ and ${}^6\text{He}$, reflecting the effect of tensor forces



Radioactive beams of energy higher than 1-2A GeV provide new opportunities to study **giant resonances** in asymmetric nuclei including a new mode (isoscalar E1)

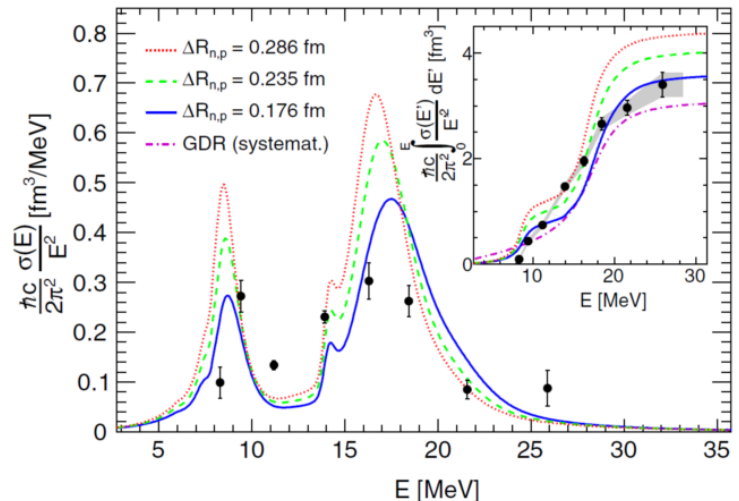


Is a neutron skin decoupled from the core?

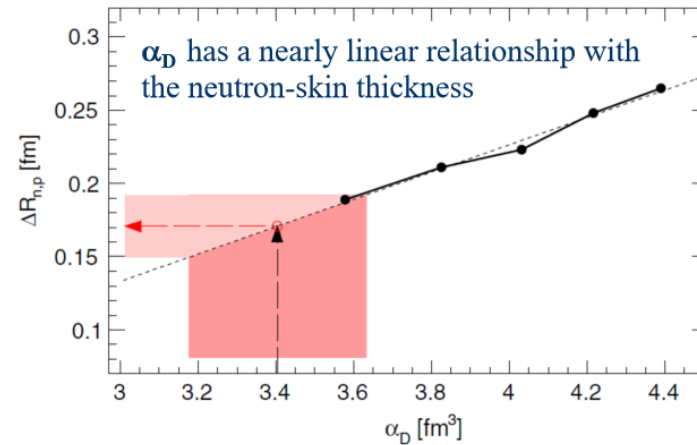
Giant dipole resonance of n-rich nuclei: a precise determination of neutron skins

- The low-lying E1 strength (PDR) in n-rich nuclei constrains the neutron-skin thickness
- The α_D is a robust and less model dependent observable to extract neutron-skin thickness

The electric dipole polarizability: $\alpha_D = \frac{\hbar c}{2\pi^2} \int_0^\infty \frac{\sigma(E)}{E^2} dE,$



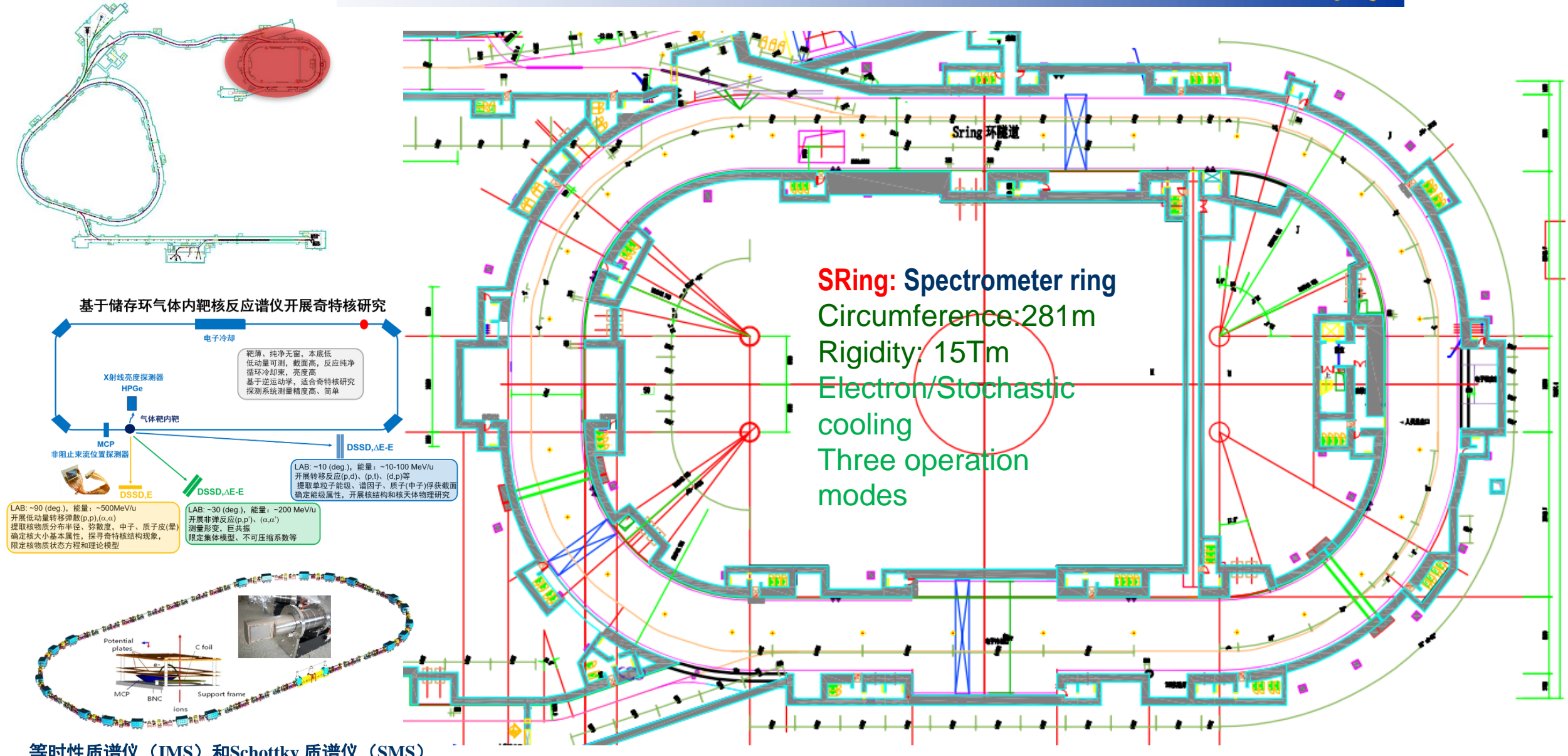
Inverse energy-weighted dipole strength for ^{68}Ni . Inset: Experimental dipole polarizability



Correlation between neutron-skin thickness and dipole polarizability in ^{68}Ni

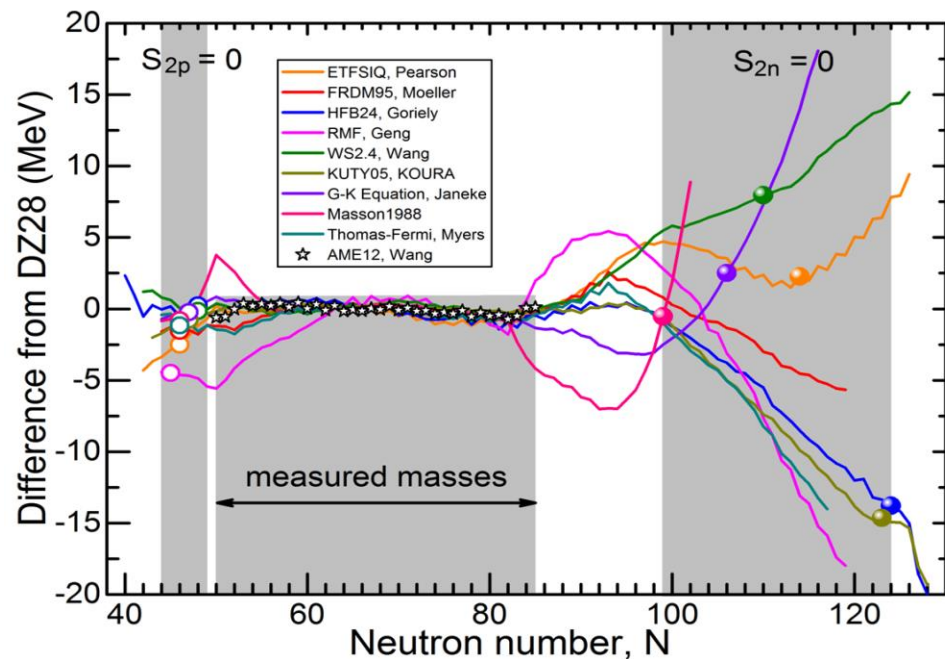
D. Rossi et al. PRL 111, 242503 (2013)

A systematic change of neutron skin thicknesses provides sensitive constraints on the EOS

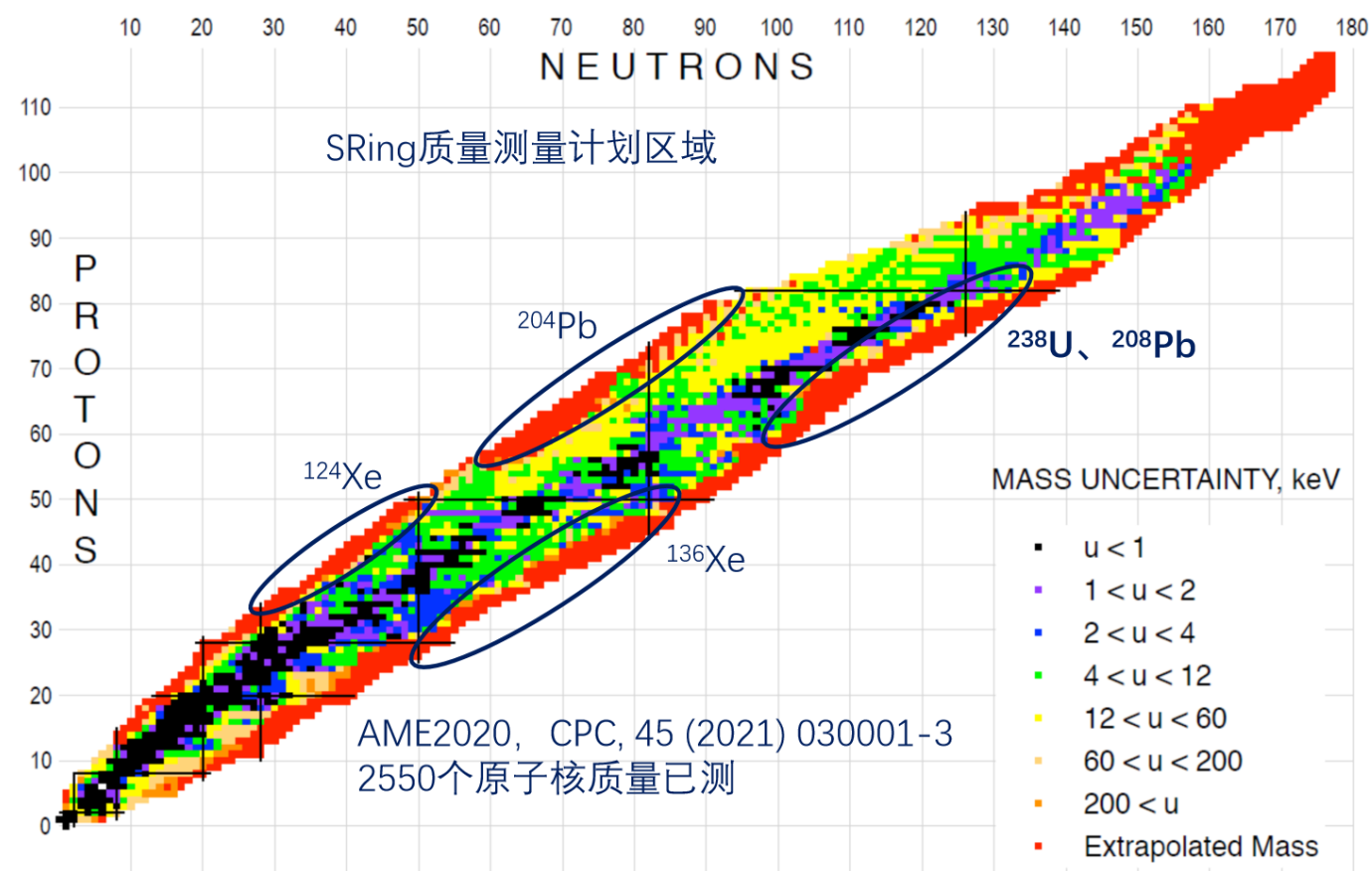


物理目标:

- 确定质子、中子滴线位置
- 研究幻数演化、发现新幻数
- 寻找高电荷态离子奇异衰变
- 模拟天体环境中核过程

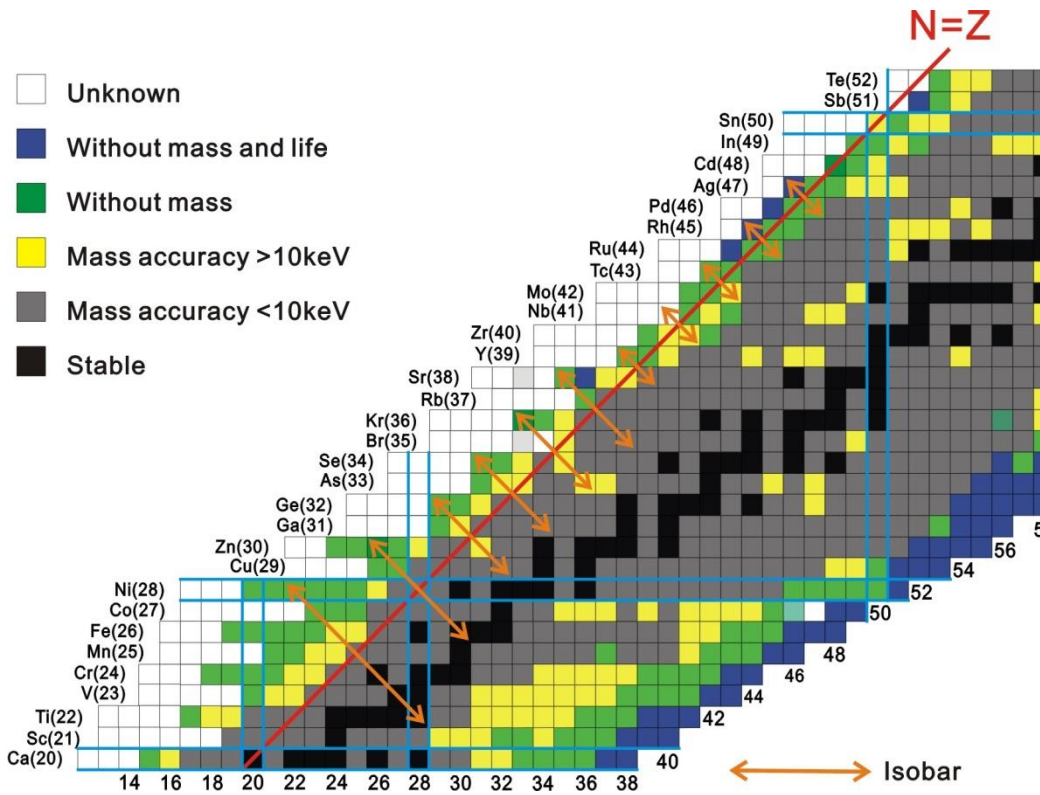


等时性质谱仪（IMS）和Schottky 质谱仪（SMS）



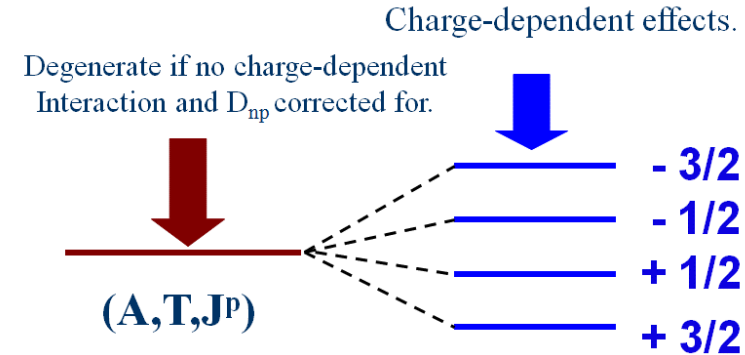
精确测量远离稳定线原子核的质量、寿命，寻找高电荷态离子的奇异衰变

Physics along the $N=Z$ line

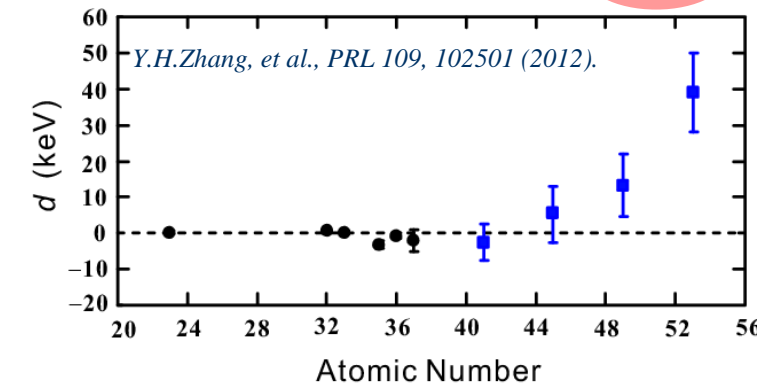


- Understanding of the *rp* process path and end point.
- Shape evolution for the nuclei along the $N=Z$ line.
- Study of the isospin symmetry breaking and its mechanisms.
- Search for the new form of *n-p* pairing.
- Precision tests of the shell model around ^{100}Sn .

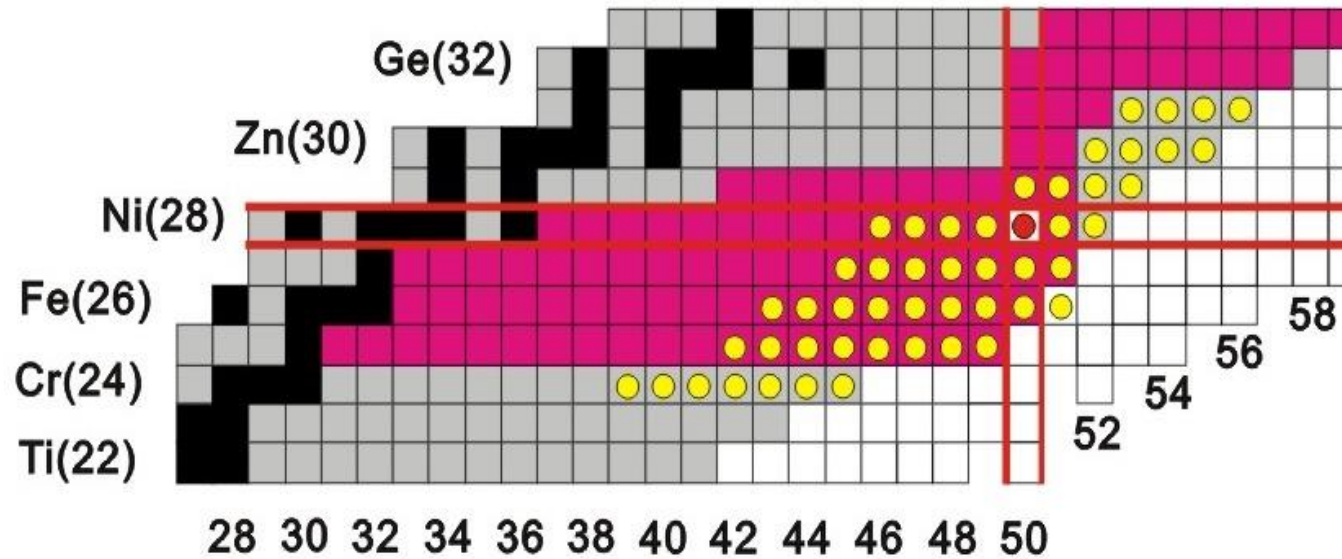
Test the Isospin Multiplet Mass Equation



$$M(T, A, T_3) = a(T, A) + b(T, A)T_3 + c(T, A)T_3^2 + d(T, A)T_3^3$$



Mass Measurements of N-rich Nuclides around ^{78}Ni



Production: Fragmentation of Projectile ^{86}Kr Using the HFRS.

Measurement: The Isochronous Mass Spectrometer with Double ToF Detectors.

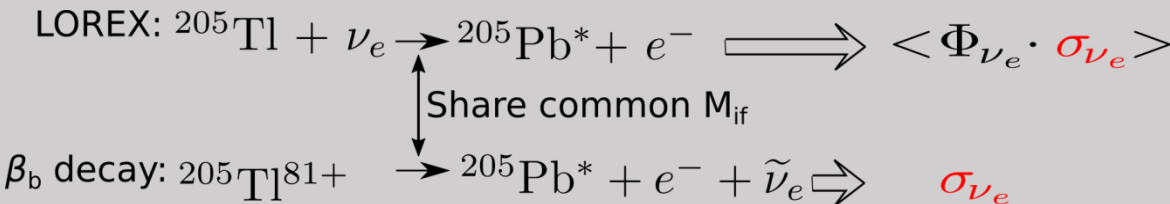
Systematically measure nuclear masses with a precision of $\sim 50\text{keV}$, and deduce one-neutron and two-neutron separation energies.

Study the evolution of the $N=50$ shell closure and Simulate the r-process.

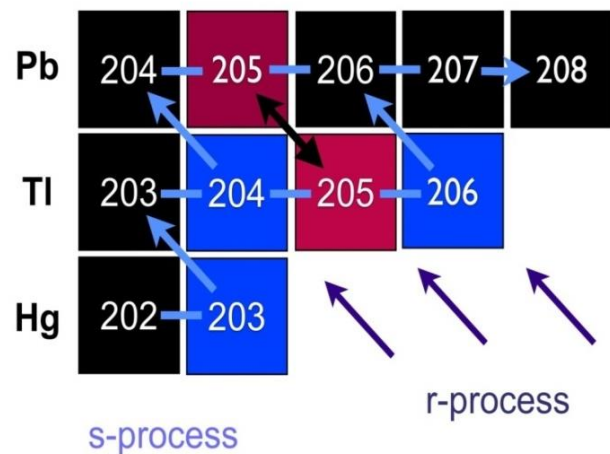
Understanding of the solar pp neutrinos

LOREX project: ^{205}Tl in lorandite at Allchar mine is used for long-time detection of solar pp neutrinos with the by far lowest threshold of neutrino energy of 52 keV.

The neutrino capture cross section σ_{ν_e} can be deduced from the half-life of bound-state β decay of $^{205}\text{Tl}^{81+}$.



Understanding of the abundance of ^{205}Pb

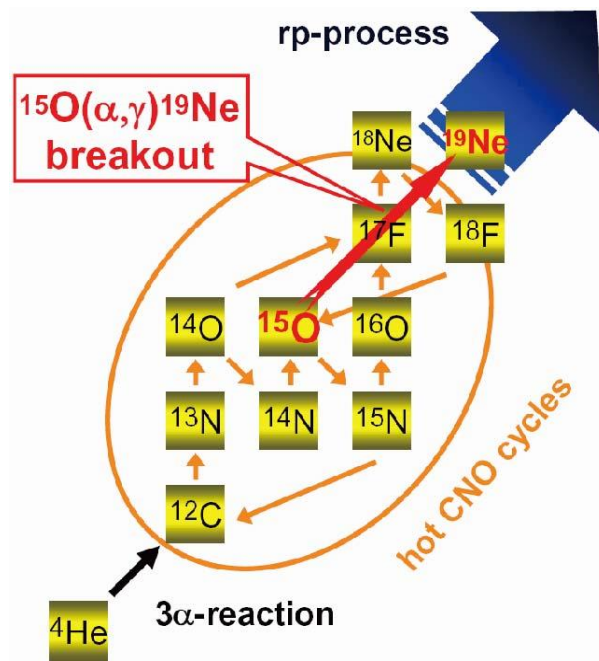


$$N(^{205}\text{Pb})/N(^{204}\text{Pb}) = P(^{205}\text{Pb})/P(^{204}\text{Pb}) \times T(^{205}\text{Pb})/T_G$$

$\sim 10^{-3}$ in inter-stellar media	~ 1 s-production ratio	$\sim 2.5 \cdot 10^{-3}$ lifetime ratio of the Galaxy
--	--------------------------------	--

In the s-process environment:
 ^{205}Pb is strongly reduced by free electron capture.
The mean lifetime of ^{205}Tl is determined by λ_{β_b} of bare ^{205}Tl .
Is ^{205}Pb counter-balanced by the β_b decay of bare ^{205}Tl ?

通过 $^{20}\text{Ne}(\text{p}, \text{d})^{19}\text{Ne}$ 研究alpha衰变分支比



突破CNO循环的关键反应

RAPID COMMUNICATIONS

PHYSICAL REVIEW C 67, 012801(R) (2003)

α -decay branching ratios of near-threshold states in ^{19}Ne and the astrophysical rate of $^{15}\text{O}(\alpha, \gamma)^{19}\text{Ne}$

B. Davids,¹ A. M. van den Berg,¹ P. Dendooven,¹ F. Fleurot,^{1,*} M. Hunyadi,¹ M. A. de Huu,¹ K. E. Rehm,² R. E. Segel,³ R. H. Siemssen,¹ H. W. Wilschut,¹ H. J. Wörtche,¹ and A. H. Wuosmaa²

¹Kernfysisch Versneller Instituut, Zernikelaan 25, 9747 AA Groningen, The Netherlands

²Physics Division, Argonne National Laboratory, Argonne, Illinois 60439

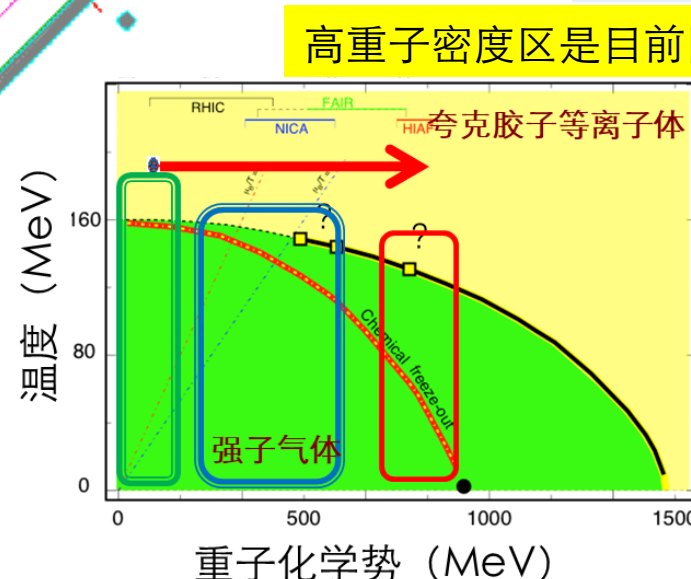
³Department of Physics, Northwestern University, Evanston, Illinois 60208

(Received 5 June 2002; published 21 January 2003)

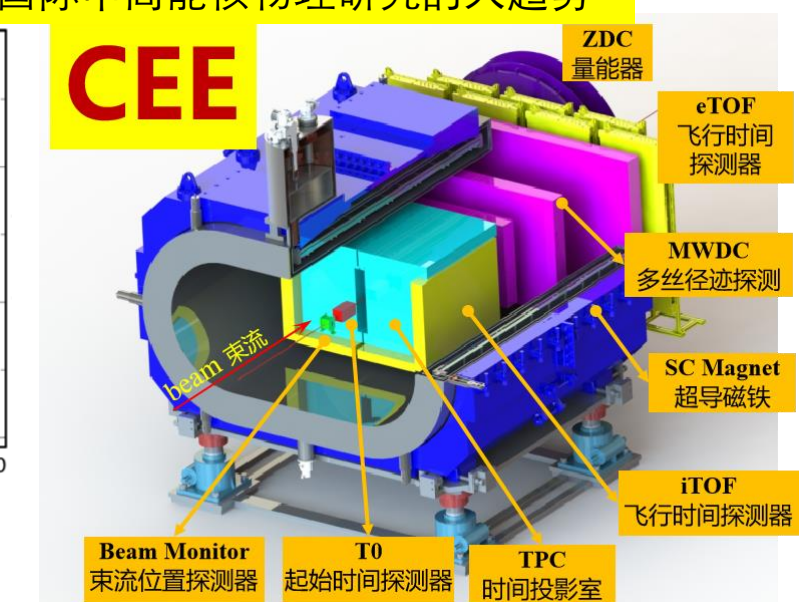
TABLE I. Branching ratios $B_\alpha \equiv \Gamma_\alpha / \Gamma$ and decay widths. Upper limits are specified at the 90% confidence level.

E_x (MeV)	J^π	B_α (present work)	B_α (Ref. [10])	B_α (Ref. [19])	B_α (adopted)	Γ_γ (meV)	Ref.	Γ_α (meV)
4.033	$\frac{3}{2}^+$	$\leq 4.3 \times 10^{-4}$			$\leq 4.3 \times 10^{-4}$	12_{-5}^{+9}	[20]	≤ 0.011
4.379	$\frac{1}{2}^+$	$\leq 3.9 \times 10^{-5}$	0.044 ± 0.032		$\leq 3.9 \times 10^{-5}$	458 ± 92	[23]	≤ 2.4
4.549	$(\frac{1}{2}, \frac{3}{2})^-$	0.16 ± 0.04	0.07 ± 0.03		0.10 ± 0.02	39_{-15}^{+34}	[18]	$4.4_{-2.0}^{+4.0}$
4.600	$(\frac{5}{2})^+$	0.32 ± 0.04	0.25 ± 0.04	0.32 ± 0.03	0.30 ± 0.02	101 ± 55	[22]	43 ± 24
4.712	$(\frac{5}{2})^-$	0.85 ± 0.04	0.82 ± 0.15		0.85 ± 0.04	43 ± 8	[18]	230 ± 80
5.092	$\frac{5}{2}^+$	0.90 ± 0.06	0.90 ± 0.09		0.90 ± 0.05	196 ± 39	[23]	1800 ± 1000

$T_9 < 0.6$ 时, 主导反应率的4.03 MeV共振能级, 尚无实验数据



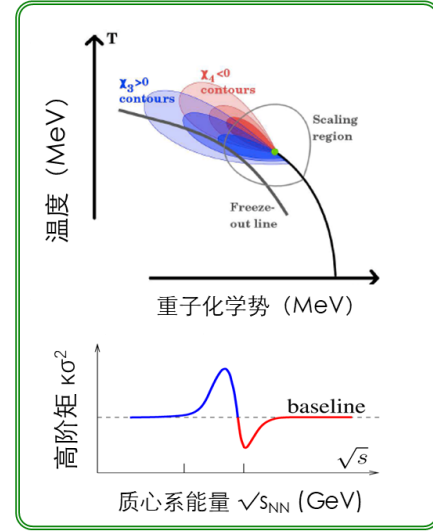
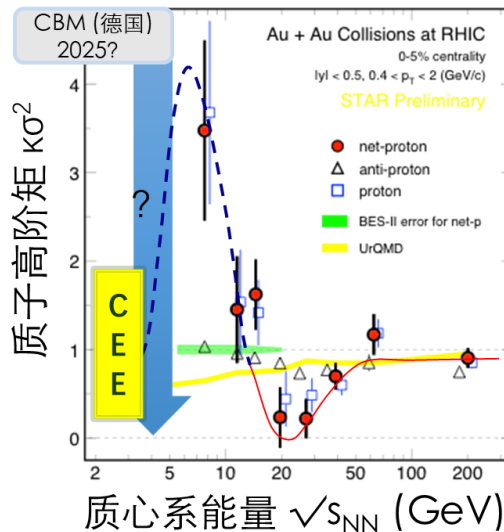
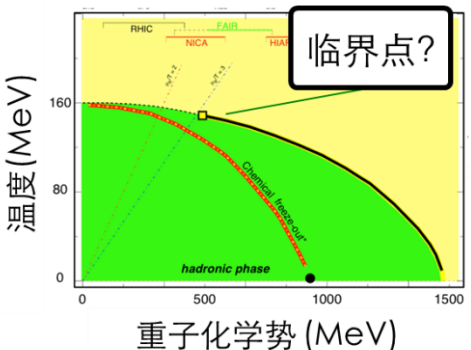
离子种类	能量(GeV/u)	流强(ppp)
P	9.3	2.0×10^{12}
$^{18}\text{O}^{6+}$	2.6	4.0×10^{11}
$^{78}\text{Kr}^{19+}$	1.7	2.5×10^{11}
$^{209}\text{Bi}^{31+}$	0.85	1.0×10^{11}
$^{238}\text{U}^{35+}$	0.8	1.0×10^{11}
$^{238}\text{U}^{76+}$	2.45	4.0×10^{10}



QCD相结构和对称能研究

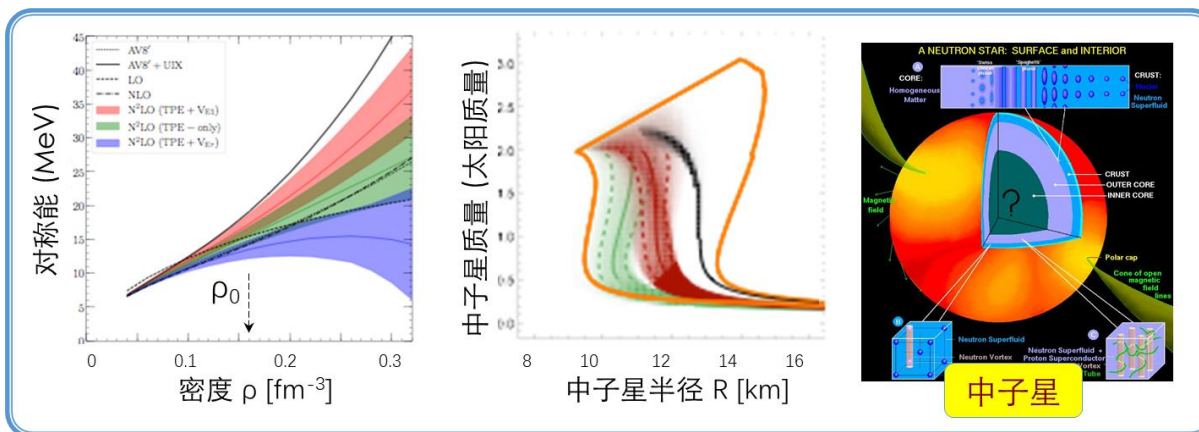
低温高密区QCD相结构(物质结构)

- 夸克禁闭
- 手征对称自发破缺
- 临界点、相边界 ...

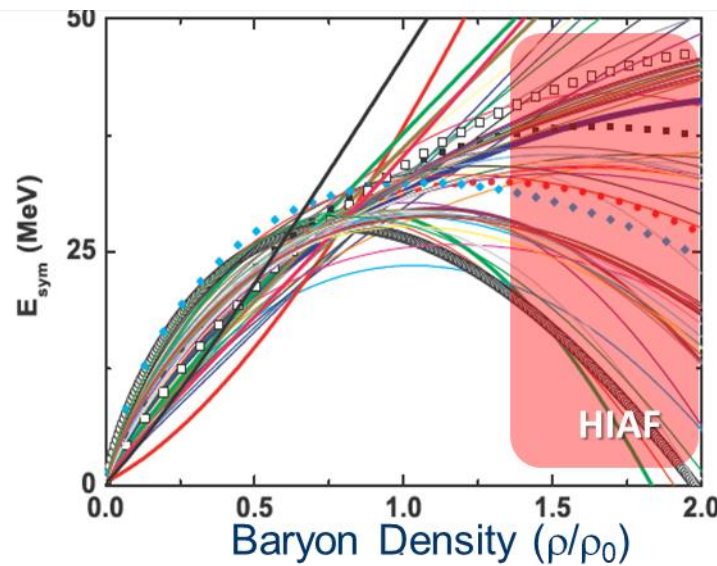


HIAF能区 +
低温高密核
物质测量谱
仪(CEE) → 为
确定QCD临
界点提供绝
佳机遇!

非对称核物质状态方程

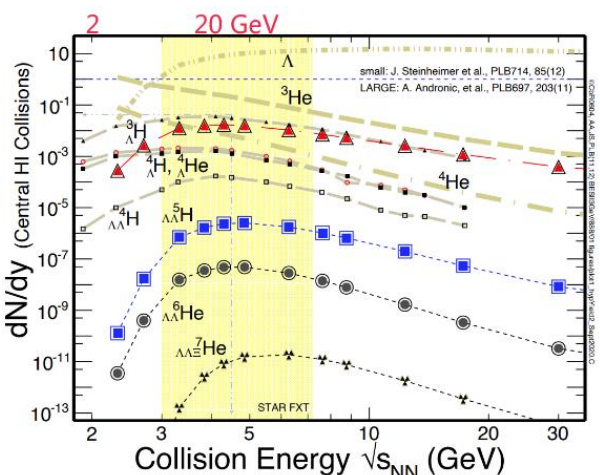
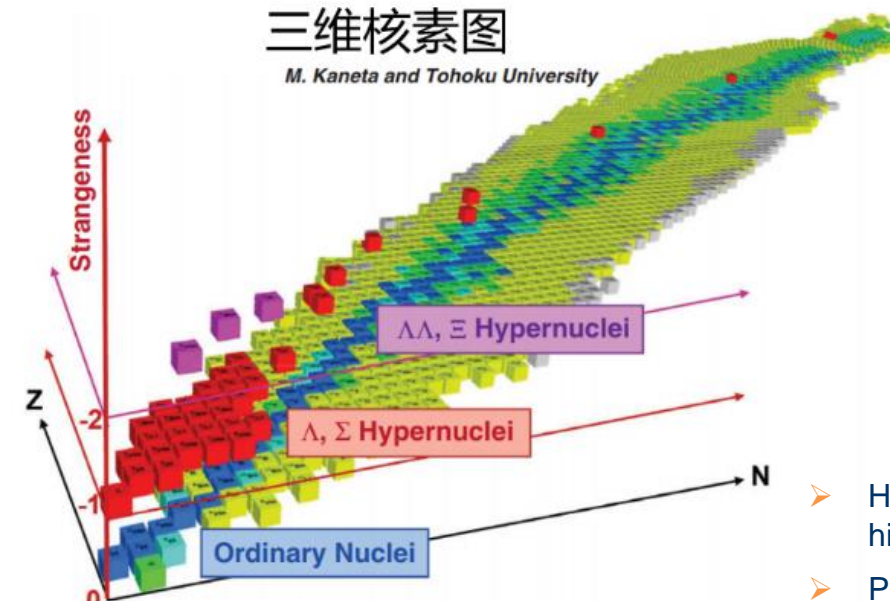


HIAF能区也是研究对称能 $E_{sym}(\rho)$ 的理想能区



三维核素图

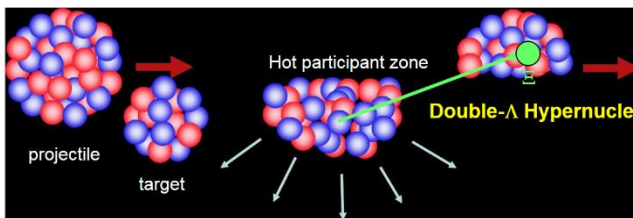
M. Kaneta and Tohoku University



重离子碰撞中超核产额和碰撞质心系能量依赖关系

Hypernuclei with Double Strangeness

发现新的超核，特别是双奇异数超核；研究超核性质、超子-核子以及超子-超子相互作用。不仅对强相互作用物质性质的理解有重要意义，也为宇宙演化、中子星结构等问题的研究提供了重要的核物理输入。



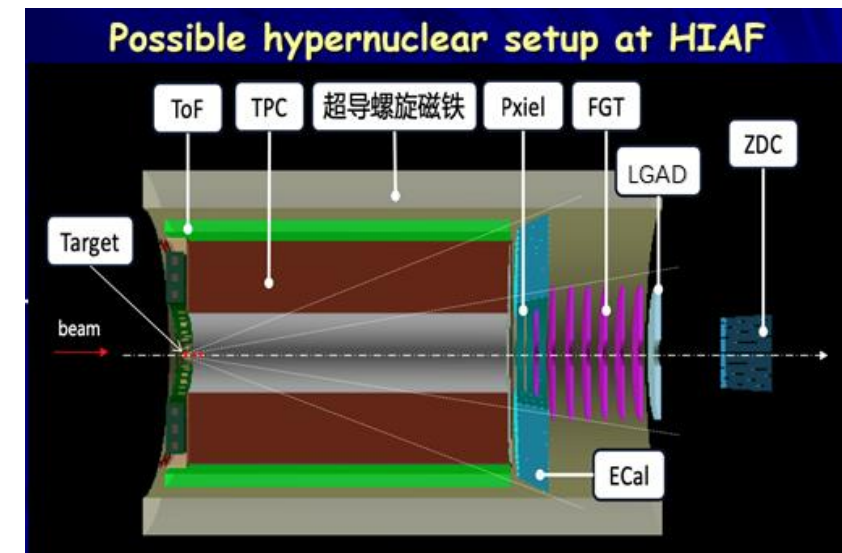
- Hypernuclei are produced by coalescence of Λ in high-energy peripheral collisions
- Production of hypernuclei is expected to have large cross sections at high-energy (>1.2 AGeV)
- In high-energy (>3.75 AGeV) collisions, double- Λ hypernuclei can be produced!

Decay of $\Lambda\Lambda$ hypernuclei

- $n\Lambda\Lambda \rightarrow {}^3He + \pi^- + \pi^-$
- $nn\Lambda\Lambda \rightarrow {}^4He + \pi^- + \pi^-$
- ${}^4_{\Lambda\Lambda}H \rightarrow p + {}^3He + \pi^- + \pi^-$
- ${}^5_{\Lambda\Lambda}H \rightarrow p + {}^4He + \pi^- + \pi^-$
- ${}^7_{\Lambda\Lambda}He \rightarrow {}^7Be + \pi^- + \pi^-$
- ${}^8_{\Lambda\Lambda}He \rightarrow {}^4He + {}^4He + \pi^- + \pi^-$
- ${}^{10}_{\Lambda\Lambda}Li \rightarrow {}^{10}B + \pi^- + \pi^-$
- ${}^{11}_{\Lambda\Lambda}Li \rightarrow {}^{11}B + \pi^- + \pi^-$
- ${}^{11}_{\Lambda\Lambda}Be \rightarrow {}^{11}C + \pi^- + \pi^-$
- ${}^{12}_{\Lambda\Lambda}Be \rightarrow {}^{12}C + \pi^- + \pi^-$

Production of $\Delta\Delta$ hypernuclei

- $d + \Xi^- \rightarrow n\Delta\Delta$
- $t + \Xi^- \rightarrow nn\Delta\Delta$
- ${}^3He + \Xi^- \rightarrow {}^4_{\Delta\Delta}H$
- ${}^4He + \Xi^- \rightarrow {}^5_{\Delta\Delta}H$
- ${}^6Li + \Xi^- \rightarrow {}^7_{\Delta\Delta}He$
- ${}^7Li + \Xi^- \rightarrow {}^8_{\Delta\Delta}He$
- ${}^9Be + \Xi^- \rightarrow {}^{10}_{\Delta\Delta}Li$
- ${}^{10}Be + \Xi^- \rightarrow {}^{11}_{\Delta\Delta}Li$
- ${}^{10}B + \Xi^- \rightarrow {}^{11}_{\Delta\Delta}Be$
- ${}^{11}B + \Xi^- \rightarrow {}^{12}_{\Delta\Delta}Be$
- ...

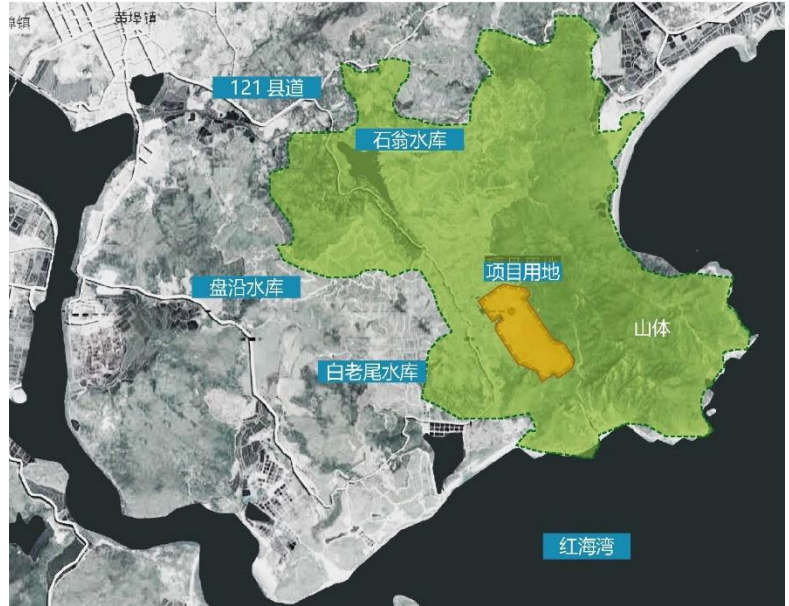


High energy & moderate intensity

Expected reconstructed rate

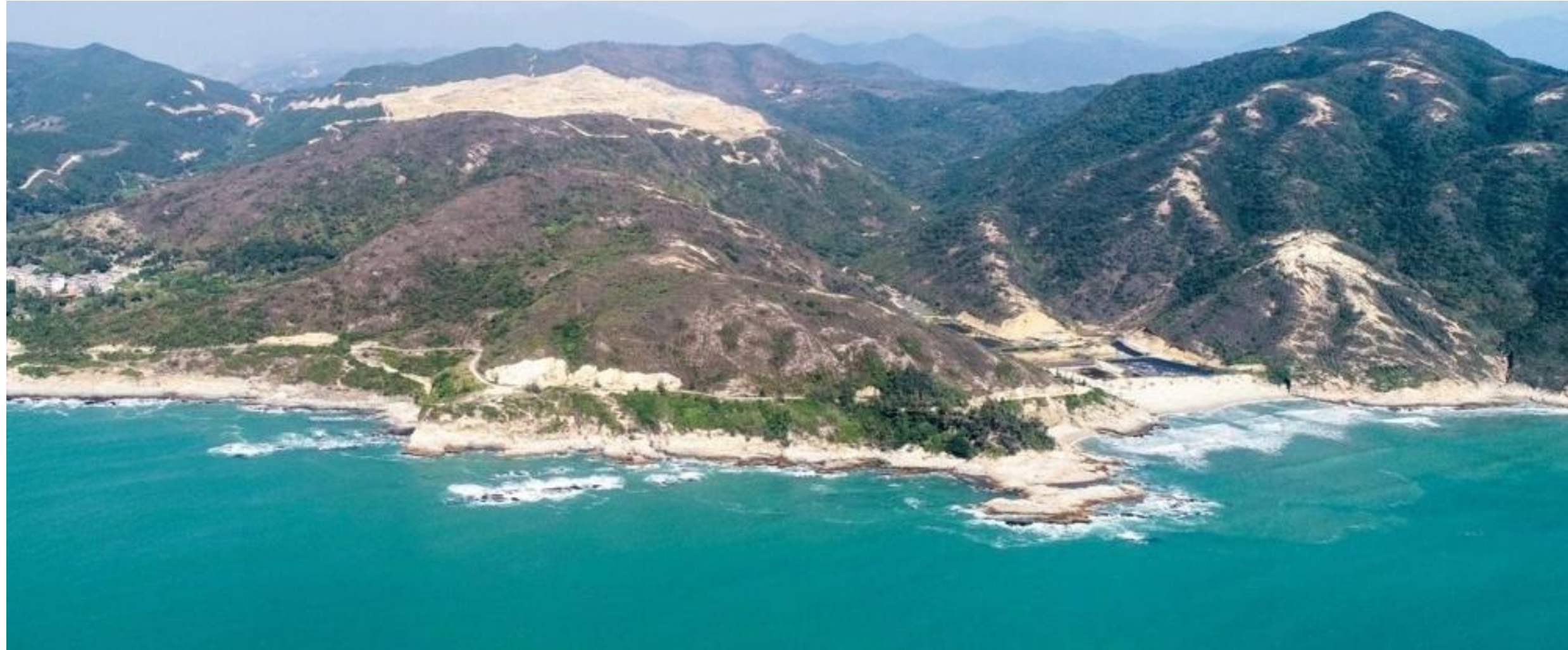
- ${}^{20}Ne + {}^{12}C$ at 4.25 A GeV
- Beam intensity: 10^7 / s

	Single- Λ hypernuclei	Double- Λ hypernuclei
per day	8×10^5	9×10^1
per week	6×10^6	6×10^2
per month	2×10^7	3×10^3





HIAF建设进展



Ground broke in August 2018



2020. 6

珠海 2022.7.3-5



HIAF建设进展





- 土石工程、水电道路等配套设施建设已经完成；
- 土建工作正在进行中，部分隧道已封顶。

■ HIAF construction time schedule

2019	2020	2021	2022	2023	2024	2025
Civil construction				Electric power, cooling water, compressed air, network, cryogenic, supporting system, etc.		
ECR design & fabrication		SECR installation and commissioning				
	Linac design & fabrication		iLinac installation and commissioning			
Prototypes of PS, RF cavity, chamber, magnets, etc.			fabrication	BRing installation & commissioning		
				HFRS & SRing installation & commissioning		
				Terminals installation		

Day One exp.

- 2022年底SECR实现供束；
- 2024年底iLinac开始供束；
- 2025年4月Bring实现束流引出。

2025年中期具备开展物理实验的条件



研究所已落户粤港澳湾区



中国科学院近代物理研究所惠州研究部

地址：惠城区新桥北路1号

今年初已经投入使用



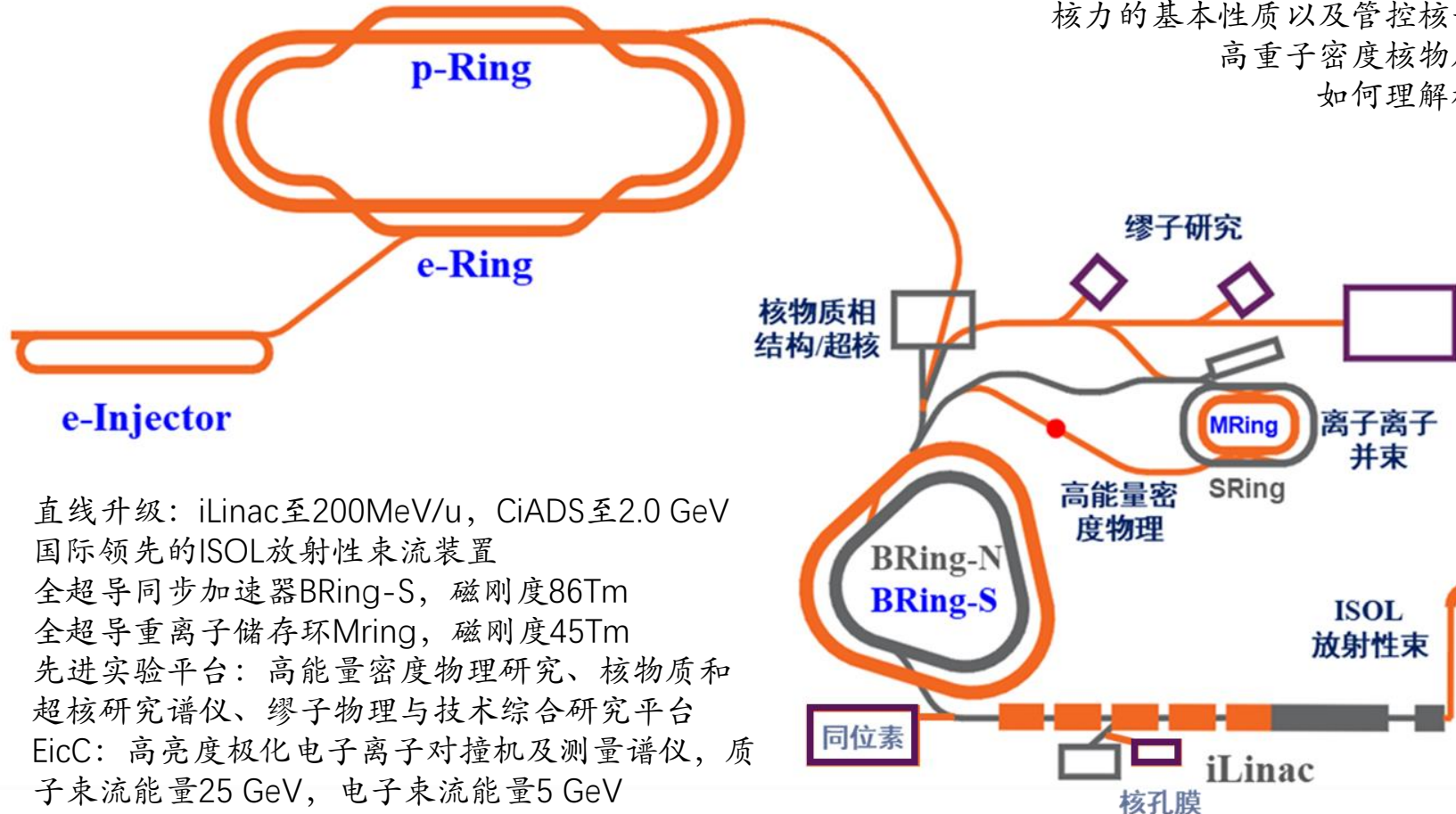
占地128亩，建筑面积5.2万平米

距离HIAF & CiADS
两装置园区约70公里



惠州核科学研究中心

电子离子对撞机



中国先进核物理研究装置
(China advanced Nuclear physics research Facility, CNUF)



Summary and Outlook



- 国家重大科技基础设施-强流重离子加速器（HIAF）将为我国核物理基础和应用研究提供一流的束流条件。
- HIAF的建设工作已在惠州全面展开，目前项目进展顺利，预期将于2025年出束。
- HIAF上的物理研究工作期盼更多国内和国际合作者的加入，希望能在研究目标确立和相关探测设备研制等方面发挥更关键的作用。
- IMP希望能够进一步深化和粤港澳大湾区同行的交流与合作，共同促进我国核物理研究的未来发展！

谢谢